

2

AD-A176 133



AFWAL-TR-86-3018

A TWO-DIMENSIONAL LINEAR ELASTIC CRACK TIP ELEMENT FOR NASTRAN

Peter J. Woytowitz
Richard L. Citerley

ANAMET LABORATORIES, INC.
3400 Investment Boulevard
Hayward, California 94545-3811

July 1986

Interim Report for Period March 1985 - May 1985

Approved for public release; distribution is unlimited.

DTIC FILE COPY

DTIC
ELECTE
JAN 21 1987
S D
E

FLIGHT DYNAMICS LABORATORY
AIR FORCE WRIGHT AERONAUTICAL LABORATORIES
AIR FORCE SYSTEMS COMMAND
WRIGHT-PATTERSON AIR FORCE BASE, OHIO 45433-6553

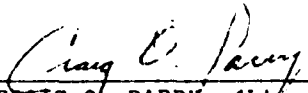
87 1 21 099

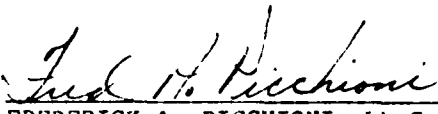
NOTICE

When Government drawings, specifications, or other data are used for any purpose other than in connection with a definitely related Government procurement operation, the United States Government thereby incurs no responsibility nor any obligation whatsoever; and the fact that the government may have formulated, furnished, or in any way supplied the said drawings, specifications, or other data, is not to be regarded by implication or otherwise as in any manner licensing the holder or any other person or corporation, or conveying any rights or permission to manufacture use, or sell any patented invention that may in any way be related thereto.

This report has been reviewed by the Office of Public Affairs (ASD/PA) and is releasable to the National Technical Information Service (NTIS). At NTIS, it will be available to the general public, including foreign nations.

This technical report has been reviewed and is approved for publication.


CRAIG O. PARRY, 1Lt, USAF
Project Engineer


FREDERICK A. PICCHIONI, Lt Col, USAF
Chief, Analysis & Optimization Branch

FOR THE COMMANDER


ROBERT M. BADER
Assistant Chief
Structures & Dynamics Division

"If your address has changed, if you wish to be removed from our mailing list, or if the addressee is no longer employed by your organization please notify AFWAL/FIBRA, Wright-Patterson AFB, OH 45433-6553 to help us maintain a current mailing list".

Copies of this report should not be returned unless return is required by security considerations, contractual obligations, or notice on a specific document.

REPORT DOCUMENTATION PAGE

1a. REPORT SECURITY CLASSIFICATION UNCLASSIFIED		1b. RESTRICTIVE MARKING ATN 133	
2a. SECURITY CLASSIFICATION AUTHORITY n/a		3. DISTRIBUTION/AVAILABILITY OF REPORT Approved for public release; distribution is unlimited.	
2b. DECLASSIFICATION/DOWNGRADING SCHEDULE n/a			
4. PERFORMING ORGANIZATION REPORT NUMBER(S) ASIAC 685.1D		5. MONITORING ORGANIZATION REPORT NUMBER(S) AFWAL-TR-86-3018	
6a. NAME OF PERFORMING ORGANIZATION Anamet Laboratories, Inc.	6b. OFFICE SYMBOL (If applicable)	7a. NAME OF MONITORING ORGANIZATION Flight Dynamics Laboratory (AFWAL/FIBRA) Air Force Wright Aeronautical Laboratories	
6c. ADDRESS (City, State and ZIP Code) 3400 Investment Blvd. Hayward, CA 94545		7b. ADDRESS (City, State and ZIP Code) Wright-Patterson AFB, OH 45433-6553	
8a. NAME OF FUNDING/SPONSORING ORGANIZATION Flight Dynamics Laboratory	8b. OFFICE SYMBOL (If applicable) AFWAL/FIBR	9. PROCUREMENT INSTRUMENT IDENTIFICATION NUMBER F33615-84-C-3216	
8c. ADDRESS (City, State and ZIP Code) Air Force Wright Aeronautical Laboratories Air Force Systems Command Wright-Patterson AFB, OH 45433-6553		10. SOURCE OF FUNDING NOS.	
11. TITLE (Include Security Classification) see reverse side		PROGRAM ELEMENT NO. 62201F	PROJECT NO. 2401
		TASK NO. 02	WORK UNIT NO. 65
12. PERSONAL AUTHOR(S) Woytowitz, P. J., and Citerley, R. L.			
13a. TYPE OF REPORT Interim Technical	13b. TIME COVERED FROM Mar 1985 to May 1985	14. DATE OF REPORT (Yr., Mo., Day) July 1986	15. PAGE COUNT 56
16. SUPPLEMENTARY NOTATION			
17. COSATI CODES		18. SUBJECT TERMS (Continue on reverse if necessary and identify by block number)	
FIELD	GROUP	SUB. GR.	
01	03		Fracture Mechanics
20	11		Crack Elements
			→ Singular Finite Elements
19. ABSTRACT (Continue on reverse if necessary and identify by block number) A new crack element has been developed and incorporated into COSMIC/NASTRAN. The element is considered linear, isotropic, and homogeneous. Mode I and II stress intensity factors are automatically calculated. Comparisons to theoretical plane strain solutions for several geometries are presented and demonstrate the accuracy of the developed element. Extensions of the element to three dimensions, anisotropic material, and plastic analysis are discussed.			
20. DISTRIBUTION/AVAILABILITY OF ABSTRACT UNCLASSIFIED/UNLIMITED <input type="checkbox"/> SAME AS RPT. <input checked="" type="checkbox"/> DTIC USERS <input type="checkbox"/>		21. ABSTRACT SECURITY CLASSIFICATION UNCLASSIFIED	
22a. NAME OF RESPONSIBLE INDIVIDUAL Lt. Craig O. Parry		22b. TELEPHONE NUMBER (Include Area Code) (513) 255-7191	22c. OFFICE SYMBOL AFWAL/FIBRA

UNCLASSIFIED

SECURITY CLASSIFICATION OF THIS PAGE

11. Title
A TWO-DIMENSIONAL LINEAR ELASTIC CRACK TIP ELEMENT FOR NASTRAN - THEORY AND
USER INSTRUCTIONS

UNCLASSIFIED

SECURITY CLASSIFICATION OF THIS PAGE

PREFACE

This report presents the theory, user instructions, and sample problems for a two-dimensional linear elastic crack tip element which was implemented into COSMIC/NASTRAN. Use of this element allows accurate calculation of stresses and stress intensity factors near a crack tip. The material is assumed to be linear elastic and isotropic in the vicinity of the crack tip.

This work was performed by the Aerospace Structures Information and Analysis Center, which is operated for the Flight Dynamics Laboratory by Anamet Laboratories, Inc. This report was prepared by Mr. Peter J. Woytowicz under Contract No. F33615-84-C-3216 and is part of Problem No. 4.2-05.

Contract F33615-84-C-3216 was initiated under Project 2401, "Structures and Dynamics," Task 240102, "Design and Analysis Methods for Flight Vehicles." The contract was administered by Mr. J. R. Johnson, AFWAL/FIBRA, Wright-Patterson AFB, OH 45433-6553.

Accession For	
NTIS GRA&I	<input checked="" type="checkbox"/>
DTIC TAB	<input type="checkbox"/>
Unannounced	<input type="checkbox"/>
Justification	
By _____	
Distribution/	
Availability Codes	
Dist	Avail and/or Special
A-1	



TABLE OF CONTENTS

	<u>Page</u>
1.0 INTRODUCTION	1
2.0 THEORETICAL DEVELOPMENT	3
2.1 ELEMENT FORMULATION	7
2.2 STIFFNESS MATRIX, MASS MATRIX AND THERMAL LOAD VECTOR	10
2.3 STRESS AND STRESS INTENSITY FACTOR CALCULATIONS ...	13
3.0 IMPLEMENTATION INTO NASTRAN	18
4.0 NUMERICAL RESULTS AND VERIFICATION PROCEDURE	20
5.0 USER INSTRUCTIONS AND SAMPLE PROBLEMS	20
5.1 REQUIRED USER INPUT AND INTERPRETATION OF OUTPUT ..	26
5.2 SAMPLE PROBLEM FOR CALCULATION OF K_I	26
5.3 SAMPLE PROBLEM FOR CALCULATION OF K_I AND K_{II}	36
6.0 SUMMARY AND CONCLUSIONS	47
REFERENCES	48
APPENDIX - MAGNETIC TAPE FORMAT AND PROCEDURE FOR INSTALLATION OF DUMMY ELEMENT CODE ON VAX COMPUTER	50

LIST OF ILLUSTRATIONS

<u>Figure</u>		<u>Page</u>
1	Nomenclature for Eight-node Isoparametric Element	8
2	Degeneration of the Eight-node Element to a Six-node Triangular Element	11
3	Element Coordinate System and Conventions for Reported Stresses and Stress Intensity Factors	14
4	Nomenclature for Crack Geometry	16
5	Element Configurations for Calculation of Stress Intensity Factors	17
6	Overview of NASTRAN Implementation for CDUM1, Singular or Non-singular Structural Element	19
7	Crack Geometries Modeled	21
8	Different Mesh Sizes Analyzed	22
9	Boundary Conditions for Edge Crack and Central Crack Specimens	23
10	Model of Central Crack in Finite Plate	25
11	ADUM1 Bulk Data Card for Singular or Non-singular Structural Element	27
12	CDUM1 Bulk Data Card for Singular or Non-singular Structural Element	28
13	PDUM1 Bulk Data Card for Singular or Non-singular Structural Element	30

LIST OF ILLUSTRATIONS (Concluded)

<u>Figure</u>		<u>Page</u>
14	Sample Problem for Calculation of K_I	32
15	Bulk Data for Model of Figure 14	33
16	Sample Problem for Calculation of K_I and K_{II}	37
17	Bulk Data for Model of Figure 16	38

LIST OF TABLES

<u>Table</u>		<u>Page</u>
1	Errors in COD and K_I as a Function of Mesh	24
2	Errors in K_I and K_{II} for 23^4 Grid Mesh	24
3	Interpretation of CDUM1 User Element Stress Output	31

1.0 INTRODUCTION

Linear elastic fracture mechanics has gained a substantial acceptance in industry and has become one of the most important design considerations. It is now well recognized that many engineering structures such as airplanes, turbines, piping (pressure vessels), bridges, etc. contain pre-existing flaws. As a result of even rather moderate service loads, crack propagation resulting from these flaws can have a dramatic effect on the service life of the component. To account for this reduction in service life, fracture mechanics analysis in conjunction with a fracture control plan is generally implemented.

The basic elements of a fracture control plan have been described by Rolfe and Barsom (Ref. 1) as follows:

1. Identification of the factors that may contribute to the structure. Description of service conditions and loadings.
2. Establishment of the relative contribution of each of these factors to a possible fracture in a member.
3. Determination of the relative efficiency and trade-offs of various design methods to minimize the possibility of failure.
4. Recommendation of specific design considerations to ensure the safety and reliability of the structure against fracture.

The life of the structural component is generally determined by the time necessary to initiate a crack and to propagate the crack from a sub-critical to critical size. Two parameters are required for successful determination: the fracture behavior of the material and the state of stress and strain around the crack tip. The three measures of the severity of stresses and strains

around the tip of cracks, typically employed in linear fracture mechanics, are the elastic stress intensity factors K_I , K_{II} , and K_{III} for the opening, the inplane shear and the anti-plane shear modes, respectively.

Numerous methods are now available for determining stress intensity factors. Tada, Paris, and Irwin (Ref. 2) present a variety of methods to predict these factors, including: boundary collocation, successive boundary stress correction, and finite element methods. The most powerful method of the three is the finite element method. A large number of papers have been written on this subject alone. Most of these are restricted to two dimensional methods and linear elastic materials.

Many of the papers written on finite elements used for fracture studies are classified as either hybrid or singular element formulations. Many of the elements developed suffered from either lack of accuracy, generality, or consistency. Barsoum (Ref. 3) points out shortcomings of several different elements. These shortcomings include inability to model rigid body or constant strain modes, inability to include thermal or body force effects, and lack of compatibility with other elements.

The discussion presented herein attempts to illustrate these shortcomings and suggests alternative two-dimensional crack element formulations that are less restrictive. This report presents the theory, implementation, instructions, and sample problems which will allow COSMIC/NASTRAN users to utilize the developed crack element. The contents of this report are as follows: Section 2 presents the theoretical development of the crack element; Section 3 describes how the crack element was implemented into COSMIC/NASTRAN; Section 4 presents various numerical results obtained using the crack element and Section 5 presents detailed user instructions and sample problems. A summary of the work performed and conclusions are presented in Section 6.

2.0 THEORETICAL DEVELOPMENT

An early concept for predicting crack propagation comes from the work of Griffith (Ref. 4) on the fracture of glass. The basic idea of his theory being that the surface of a solid possesses surface tension, similar to liquids; thus, when a crack in a solid propagates, the increase in externally added or internally released energy is balanced by the increase in surface tension energy. If in an elastic solid, V and U represent, respectively, the work of the externally applied forces and the strain energy, and if the specific surface tension energy is denoted by γ , then Griffith's energy balance criterion, as shown by Reference 5, may be expressed as follows:

$$\frac{d}{dA} (V - U) = \gamma \quad (1)$$

It is pointed out that the foregoing energy-balance relation is only a necessary condition for crack growth, with the quantity on the left-hand side representing the energy available for fracture, and the quantity on the right hand side, the resistance of the solid to fracture propagation. From this physical meaning of the terms involved in the energy-balance equation, it also follows that the stability of quasi-fracture propagation may be determined from:

$$\begin{aligned} \frac{d}{dA} \left[\frac{d}{dA} (V - U) - \gamma \right] &> 0 : \text{unstable crack growth} \\ &= 0 : \text{neutral equilibrium} \\ &< 0 : \text{stable crack growth} \end{aligned} \quad (2)$$

Based on the asymptotic solutions to crack problems presented by Westergaard and Sneddon (Refs. 6 and 7), Irwin (Ref. 8) gave the name of "stress intensity factor" to the coefficient which appears in the asymptotic expression for stress. Irwin noted that the energy available for fracture per unit crack extension may be directly related to that coefficient by:

$$\frac{d}{da} (U - V) = G = K^2/E^* \quad (3)$$

Where the quantity G (after Griffith), introduced by Irwin, is known as the "strain energy release rate." Subsequently, Irwin showed that the stress and displacement fields around a crack tip in a linearly elastic solid under the most general loading conditions may be expressed in terms of three stress intensity factors: K_1 , K_2 , and K_3 , associated, respectively, with the opening, in-plane shear and anti-plane shear modes of deformation.

Generalizing Irwin's findings for linear materials, the asymptotic expressions for stresses and displacements near the tip of a crack have the following form:

$$\sigma_{1j} = \frac{k_1(t)}{r^\alpha} f_{1j}^1(\theta, C_k) + \frac{k_2(t)}{r^\alpha} f_{1j}^2(\theta, C_k)$$

$$u_1 = \frac{1}{E^*} k_1(t) r^{1-\alpha} F_1^1(\theta, C_k) + \frac{1}{E^*} k_2(t) r^{1-\alpha} F_1^2(\theta, C_k)$$

$$\text{for: } 0 < \alpha < 1 ; \quad 1, j = x, y$$

and

$$\sigma_{1z} = \frac{k_3(t)}{r^\beta} f_{1z}^3(\theta, C_k) ; \quad 0 < \beta < 1 ; \quad i = x, y$$

$$u_z = \frac{1}{\mu^*} k_3(t) r^{1-\beta} F_3(\theta, C_k) \quad (4)$$

where E^* and μ^* are normalizing material moduli; the C_k are dimensionless material constants; and f_{1j}^k and F_1^k are known, bounded functions. Also, for clarity, the following notation has been used:

$$k_1 = K_1 / \sqrt{\pi} \quad (5)$$

In the previous expressions, the powers α and β of the singularities differ from 1/2 only in nonhomogeneous and in certain homogeneous but anisotropic materials.

Quite naturally, in dynamic problems, the stress intensity factors, K_1 are functions of time and are defined, following Irwin, as the coefficients of the singular terms in the expressions for stresses; thus, for Mode I type of loading, for example:

$$k_1(t) \stackrel{\text{def}}{=} \frac{1}{f_{yy}^I(0, C_k)} \lim_{r \rightarrow 0} r^\alpha \sigma_{yy}(r, 0, 0, t) \quad (6)$$

Practical use of the previous concepts is possible when the resistance to fracture of the material is known. Hence, if in Mode I fracture, G is used to characterize the material, the necessary condition for fracture becomes:

$$G_1 = G_{1c} \quad (7)$$

where G_{1c} , the critical resistance parameter, is known as the "critical strain energy release rate" in Mode I. Similarly, if the corresponding critical value of K_1 is used to represent the material's resistance to fracture, the fracture criterion becomes:

$$K_1 = K_{1c} \quad (8)$$

in any event, since G_{1c} and K_{1c} , being material parameters, are constant, the stability of crack growth would be determined from dG_1/da and dK_1/da , respectively.

More generally, under three-dimensional loading conditions all three modes of deformation mentioned above are present and

since G is a scalar quantity, the total energy available for fracture is given by:

$$G = G_1 + G_2 + G_3 \quad (9)$$

with the new incremental crack surface, dA , lying in the plane that corresponds to the maximum available energy, G , provided the material is isotropic with regard to fracture resistance.

In addition, fracture criteria in terms of stress intensity factors usually adopt the form of interaction envelopes as shown by References 9 and 10, either

$$\left(\frac{K_1}{K_{1c}}\right)^2 + \left(\frac{K_2}{K_{2c}}\right)^2 + \left(\frac{K_3}{K_{3c}}\right)^2 = 1 \quad (10)$$

or

$$a_{11}K_1^2 + 2a_{12}K_1K_2 + a_{22}K_2^2 + a_{33}K_3^2 = 1 \quad (11)$$

as suggested by Erdogan and Sih (Ref. 11) and by Sih (Ref. 12) based on energy arguments.

Based on the foregoing presentation, it is only natural that two basic approaches have been followed to ascertain the fracture behavior of linear elastic solids containing cracks:

1. determination of stress intensity factors
2. determination of strain energy release rate

Both methods are essentially equivalent.

For the present case, the determination of the stress intensity factors for a two dimensional system using finite element formulation will be considered. Other authors have suggested some of the shortcomings of earlier finite elements developed for fracture mechanics studies. The elements developed by Barsoum

(Ref. 3) and Henshell and Shaw (Ref. 13) rectified many of the problems described above; however, these elements were limited to displacement of the form $r^{1/2}$. Consequently, they could only model strain singularities of the form $r^{-1/2}$. Recently, Stern (Ref. 14) and more recently, Hughes and Akin (Ref. 15) introduced families of consistent, conforming elements which allow displacements of the form r^γ . While the Stern element appears to have the restriction that $0 < \gamma < 1$, the element of Hughes and Akin is valid for all $\gamma > 0$. The element described herein is based upon shape functions suggested by Hughes and Akin.

The element presented here possesses the required rigid body and constant strain modes. It properly models thermal, body force, and pressure loading conditions. Additionally, it is compatible with standard linear or quadratic isoparametric elements and can be used as a nonsingular element with a variable number of nodes.

The following sections present the element formulation. This includes the assumed shape functions, procedures for calculating the stiffness and mass matrices, and equivalent thermal loads. Also, the equations used to evaluate stresses and stress intensity factors are presented.

2.1 ELEMENT FORMULATION

The following derivation follows Hughes and Akin. Referring to Figure 1, the standard bilinear shape functions are used for grids 1 through 4:

$$\begin{aligned} N_1(r,s) &= (1-r)(1-s) \\ N_2(r,s) &= r(1-s) \\ N_3(r,s) &= rs \\ N_4(r,s) &= (1-r)s \end{aligned} \tag{12}$$

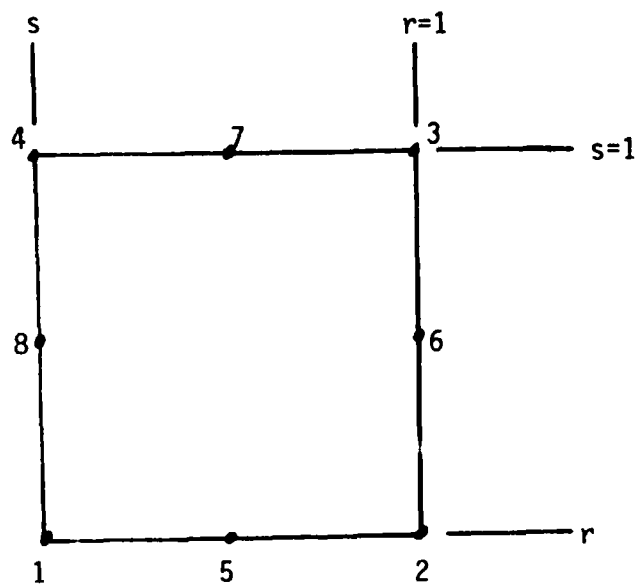


Figure 1 Nomenclature for eight-node isoparametric element.

The shape functions for grids 5 - 8 are chosen as:

$$\begin{aligned}
 N_5(r,s) &= (1-s)P(r,\gamma) \\
 N_6(r,s) &= rP(s,\gamma) \\
 N_7(r,s) &= sP(r,\gamma) \\
 N_8(r,s) &= (1-r)P(s,\gamma)
 \end{aligned}
 \tag{13}$$

where

$$P(x,\gamma) = 2 \left(x - \frac{x^\gamma - 2(1/2)^\gamma x}{1 - 2(1/2)^\gamma} \right)
 \tag{14}$$

It can be easily shown that the shape functions for grids 5 - 8 reduce to the standard quadratic serendipity element when γ of Equation (14) is set equal to 2. It can also be observed that the shape function for grids 5 - 8 satisfies the interpolation property at all nodes of the element. That is:

$$N_1(r_j) = \delta_{1j} \text{ and } N_1(s_j) = \delta_{1j}$$

where r_j and s_j are values of r and s at grid j , and δ_{1j} is the Kronecker delta. However, the shape functions associated with grids 1 - 4 do not satisfy the interpolation property at grids 5 - 8. Following the standard technique (Ref. 15) the shape functions for grids 1 - 4 are modified as follows:

$$\begin{aligned}
 N_1 + N_1(r,s) &- [N_8(r,s) + N_5(r,s)]/2 \\
 N_2 + N_2(r,s) &- [N_5(r,s) + N_6(r,s)]/2 \\
 N_3 + N_3(r,s) &- [N_6(r,s) + N_7(r,s)]/2 \\
 N_4 + N_4(r,s) &- [N_7(r,s) + N_8(r,s)]/2
 \end{aligned}
 \tag{15}$$

where the + reads: "is replaced by".

It can be shown that the shape functions for all eight grids satisfy the required interpolation property. Additionally, the shape functions are capable of exactly representing the monomials

1, r, s, r^γ , rs, s^2 , $r^\gamma s$, and $s^2 r$. The presence of 1, r, and s ensure representation of rigid body and constant strain modes. The presence of r^γ allows exact representation of displacements of the form r^γ . Note that this will result in a line singularity of the form $r^{\gamma-1}$ upon differentiation.

In order to represent point singularities, the quadrilateral form is degenerated into a triangle. This is done by coalescing grids 4, 8, and 1 as can be done for standard isoparametric elements (Ref. 16) and as is shown schematically in Figure 2. Thus, for a point singularity, the shape function associated with grid 1 is replaced with:

$$N_1(r,s) + N_1(r,s) + N_4(r,s) + N_8(r,s) \quad (16)$$

In summary, for the 6-grid triangle, the shape function associated with grid 1 is given by Equation (16), the shape functions associated with grids 2 and 3 are given by N_2 and N_3 of Equation (15), and the shape functions associated with grids 5 through 7 are given by N_5 through N_7 of Equation (13).

When the 6-grid triangle is used and γ of Equation (14) is set appropriately, then a singular element or crack element is developed. If γ is set equal to 2, then the standard serendipity element (Ref. 17) is obtained. Additionally, if $\gamma = 2$, any of the mid-side grids may be omitted. This element can then be used as a transition element to change from a mesh of quadratic elements to one of linear elements. If the singular triangular element is used (Figure 2), then the only grid which may be eliminated from Figure 2 is grid 6. User instructions for eliminating the mid-side grids will be presented in Section 5.

2.2 STIFFNESS MATRIX, MASS MATRIX AND THERMAL LOAD VECTOR

Given the shape functions of the previous section, calculation of the element's stiffness matrix, mass matrix, and thermal load vector follows the standard procedure as described in

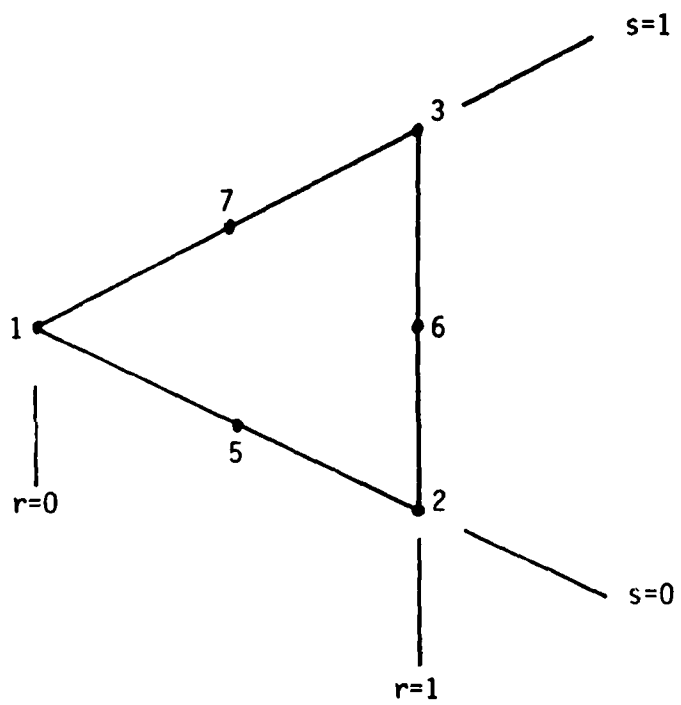


Figure 2 Degeneration of the eight-node element to a six-node triangular element.

Reference 17. These quantities are given in terms of element coordinates as

$$\underline{K}^e = \int_{V^e} \underline{B}^T \underline{D} \underline{B} dV$$

$$\underline{M}^e = \int_{V^e} \rho \underline{N}^T \underline{N} dV$$

$$\underline{P}_T^e = \int_{V^e} \underline{B}^T \underline{D} \underline{g} \Delta T dV \quad (17)$$

where

$$\underline{B} = \underline{L} \underline{N}, \quad \underline{N} = [N_1 \underline{I}, N_2 \underline{I}, \dots, N_n \underline{I}], \quad \underline{L} = \begin{bmatrix} \frac{\partial}{\partial x} & 0 \\ 0 & \frac{\partial}{\partial y} \\ \frac{\partial}{\partial y} & \frac{\partial}{\partial x} \end{bmatrix}, \quad \underline{g} = \begin{bmatrix} \alpha \\ \alpha \\ 0 \end{bmatrix}$$

\underline{I} is a 2 by 2 identity matrix and the definition of \underline{D} will be given in Section 2.3. See Reference 17 for more details. The integrations are performed using Gaussian quadrature. That is, the integrals are approximated as:

$$\int f(x) dx \approx \sum_{j=1}^n W_j f(a_j) \quad (18)$$

Due to the formulation, it can be shown that along the s direction, the integration order needs to be, at most, 4 to exactly integrate the element. For singular forms of the element, the integration order recommended along the s direction is 4 and along the r direction is 5. If the element is used in a non-singular form, then 2 by 2 integration is recommended for undistorted or slightly distorted elements, and 3 by 3 integration is recommended for distorted elements (Ref. 16).

2.3 STRESS AND STRESS INTENSITY FACTOR CALCULATIONS

For the present element, stresses are calculated and reported at the natural coordinate centroids. These correspond to the locations of $s = r = 1/2$ in Figures 1 and 2. The stresses are calculated using the equations

$$\underline{\sigma} = \underline{D} \underline{\epsilon} = \underline{D} \underline{B} \underline{u}^e$$

where

$$\underline{D} = \begin{bmatrix} (\lambda+2\mu) & \lambda & 0 \\ \lambda & (\lambda+2\mu) & 0 \\ 0 & 0 & \mu \end{bmatrix}$$

\underline{u}^e are the element's grid displacements, and \underline{B} was defined in Section 2.2. This D matrix is for plane strain. For plane stress, λ is replaced by $2\lambda\mu/(\lambda+2\mu)$.

In addition to the stresses, the element coordinates of these stress locations are also reported. These x and y locations are measured in element coordinates as depicted in Figure 3. The x and y locations are given by:

$$x = \sum_1 N_1 x_1^e$$

$$y = \sum_1 N_1 y_1^e$$

where x_1^e and y_1^e are the coordinates of the element's grid points measured in element coordinates and the summation is carried out over the number of grid points. The shape functions, N_1 , are evaluated at $s = r = 1/2$.

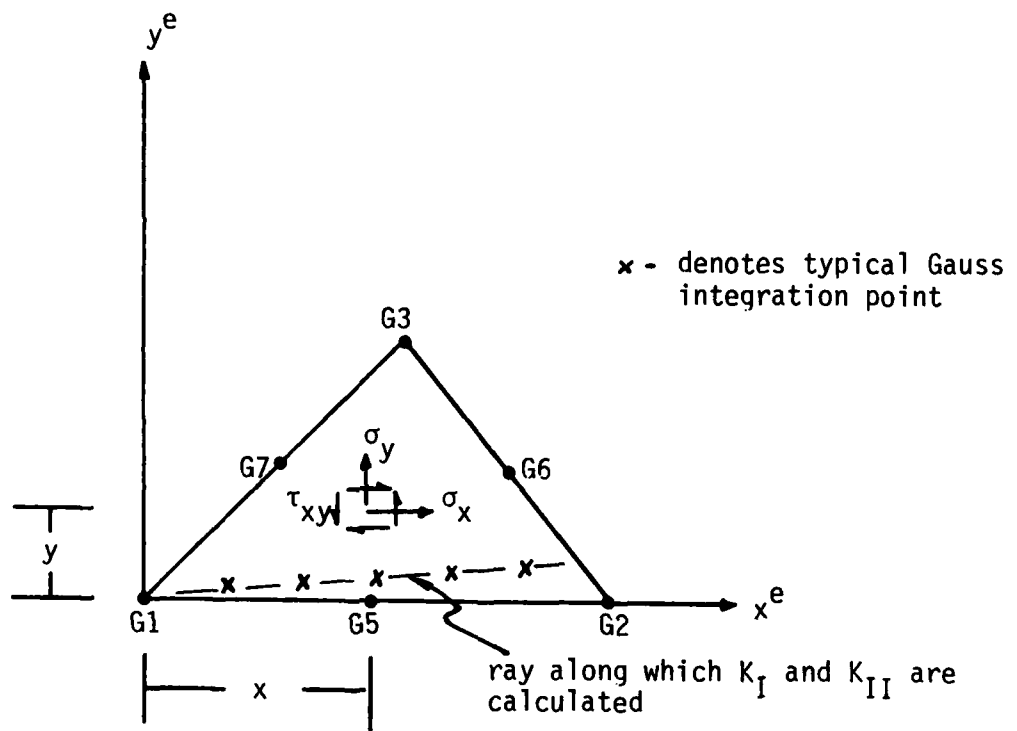


Figure 3 Element coordinate system and conventions for reported stresses and stress intensity factors.

The stress intensity factors calculated are based upon the stress or displacement fields of the crack element. When the calculations are based on stresses, the resulting equations are:

$$K_I = \lim_{r \rightarrow 0} (2\pi r)^{1/2} \sigma_y(\theta=0)$$

$$K_{II} = \lim_{r \rightarrow 0} (2\pi r)^{1/2} \tau_{xy}(\theta=0) \quad (19)$$

where the nomenclature is shown in Figure 4. If the stress intensity factors are based on displacements, the equations used are:

$$K_I = \frac{\mu}{2(1-\nu)} \lim_{r \rightarrow 0} \left(\frac{2\pi}{r}\right)^{1/2} u_y(\theta=\pi)$$

$$K_{II} = \frac{\mu}{2(1-\nu)} \lim_{r \rightarrow 0} \left(\frac{2\pi}{r}\right)^{1/2} u_x(\theta=\pi) \quad (20)$$

Equation (20) is for plane strain. For plane stress, ν is replaced by $\nu/(1+\nu)$.

The limits of Equations (19) and (20) are determined by evaluating the expression on the right hand side of the limit sign at the Gauss integration points along the ray nearest the grid 1-2 edge depicted in Figure 3. The expressions on the right hand side of the limit signs are then extrapolated to $r = 0$ using Lagrangian interpolation.

If the stress intensities are based upon displacements (Equation (20)), then the crack element configuration must be as shown for Element 1 in Figure 5a. If the stress intensities are based on stresses (Equation (19)), the crack element configuration must be as shown for Element 4 in Figure 5b. Further instructions regarding calculations of stress intensities are presented in Section 5.

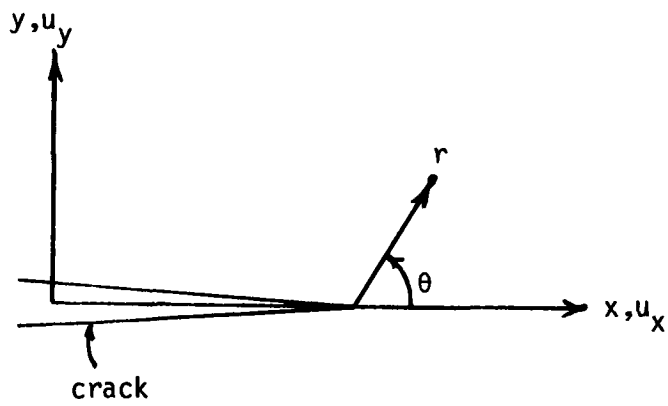
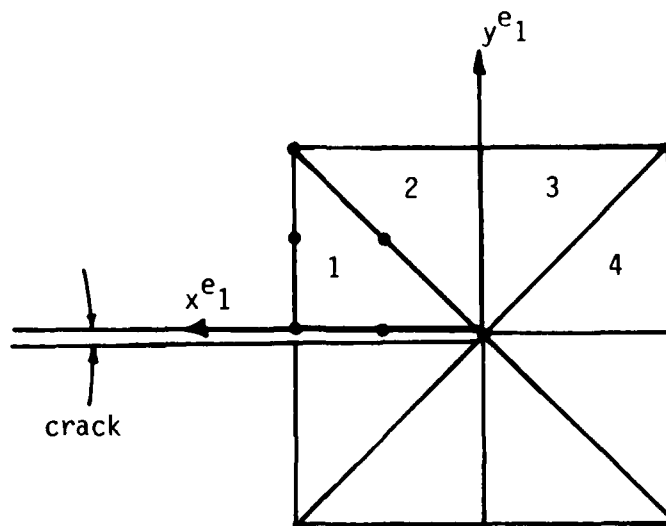
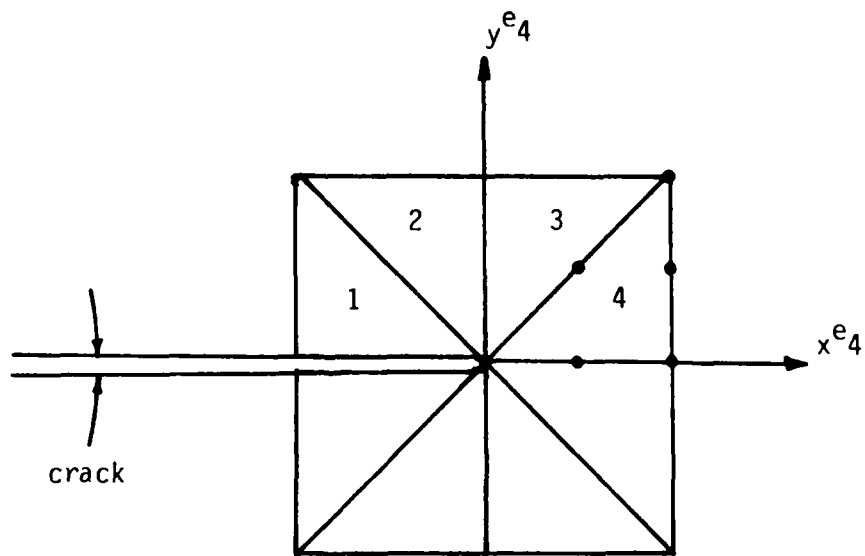


Figure 4 Nomenclature for crack geometry.



(a) Stress intensity factors for Element 1 must be based on displacements ($IKI = 1$)



(b) Stress intensity factors for Element 4 must be based on stresses ($IKI = 0$)

Figure 5 Element configurations for calculation of stress intensity factors.

3.0 IMPLEMENTATION INTO NASTRAN

Implementation of the crack element into NASTRAN was performed via the dummy element CDUM1. This procedure is discussed more completely in Reference 18. The present element was modeled after the CIS2D8 element routines, due to their similarity.

The first step was to create a subroutine KDUM1 which generates the stiffness and mass matrices. The mass matrix may be either consistent or lumped. When the mass matrix is used for calculation of gravity loads, the consistent mass matrix should be specified. This subroutine is eventually linked to NASTRAN LINK 8.

For computation of thermal loads, the subroutine EDTL must be modified to make a call to SSGETD before calling the routine DUM1. The dummy coding in routine DUM1 is then modified to calculate the thermal load vector based on the average element temperature. After EDTL and DUM1 have been modified, they must be linked to NASTRAN LINK 5.

Finally, the dummy coding for the SDUM11 and SDUM12 routines must be modified so that it performs the required operations. SDUM11 performs the preliminary geometry calculations and creates various data arrays to be used in Phase 2 stress recovery. SDUM12 then uses these data arrays, grid point displacements, and temperatures to compute stresses and stress intensity factors and writes them to the output file. After the SDUM11 and SDUM12 coding has been modified, it is linked to NASTRAN LINK 13.

An overview of the various routines and their functions is presented in Figure 6. These subroutines must be compiled and linked to the NASTRAN executable code. Instructions for compiling and generating the new NASTRAN executable code on a VAX computer are presented in the appendix.

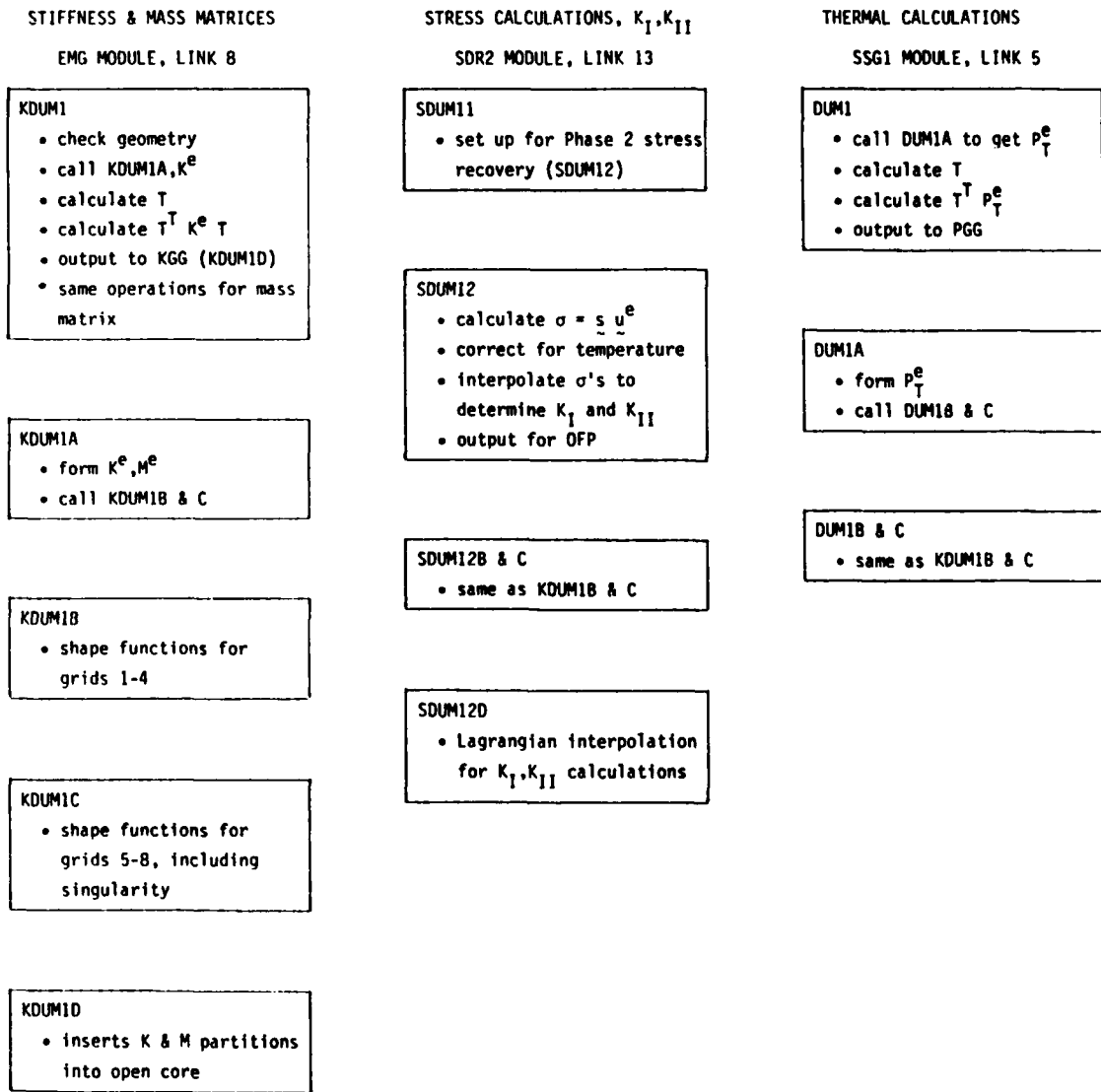


Figure 6 Overview of NASTRAN implementation for CDUM1, singular or non-singular structural element.

4.0 NUMERICAL RESULTS AND VERIFICATION PROCEDURE

To assess the accuracy of the present element, four different crack geometries/loading conditions with known solutions were analyzed. Figure 7 shows the different geometries analyzed. Figure 8 presents four different mesh sizes which were used to analyze the first three crack geometries. Figure 9 shows the boundary conditions used. For the edge crack with a point load, Figure 9 is modified so that the load is applied at the edge of the crack. Table 1 presents the errors associated with both the crack opening displacement (COD) and the mode I stress intensity factor K_I . As can be seen, the COD is less sensitive to the mesh size, while the K_I values appear to be converging to their exact solutions. However, the edge crack with a point load solution appears to overshoot the exact solution by about 5%. It should be mentioned that the "exact" solution for the edge crack specimen with a point load is considered to be accurate to within 2%. The other solutions were considered to have accuracies better than 1%. These solutions were obtained from Reference 2.

Figure 10 presents a model of a central crack in a finite plate. To ascertain the accuracy of the element's mode II stress intensity factor, K_{II} , the model of Figure 10 was used. The results for both K_I and K_{II} are presented in Table 2. As can be seen, the K_{II} is within about 4% of the exact solution.

In addition to the test cases previously described, various simple patch tests were performed to ensure proper coding of the element routines. These tests include rigid body motion tests, free thermal expansion tests, and simple uniaxial and biaxial loading configurations. The element performed properly, passing all tests.

5.0 USER INSTRUCTIONS AND SAMPLE PROBLEMS

The following sections present the required user input and detailed instructions for using the developed crack element. The first problem uses a fairly crude mesh to calculate the K_I stress

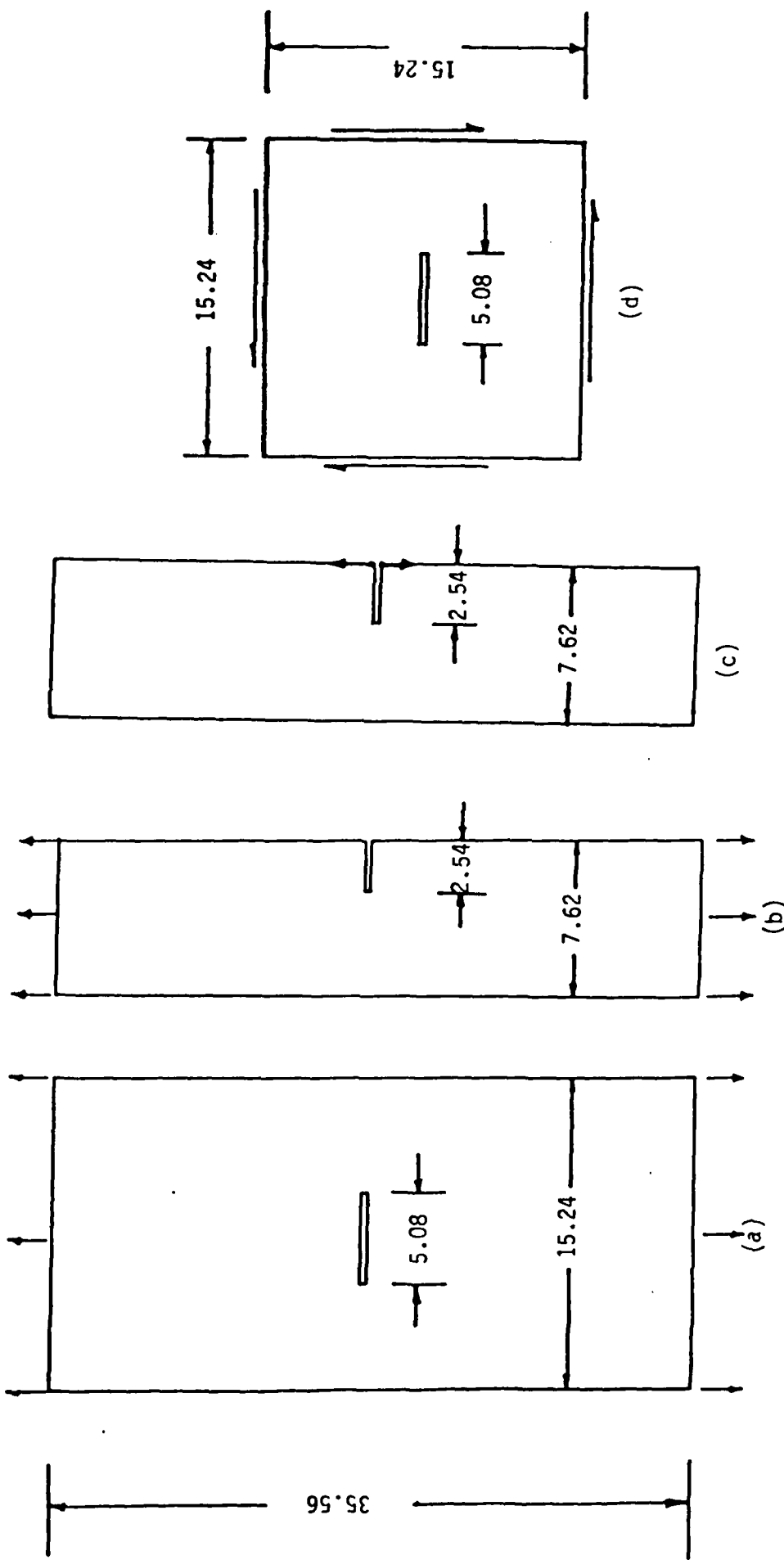


Figure 7 Crack geometries modeled (dimensions in cm's).
 (a) central crack
 (b) edge crack, uniform load
 (c) edge crack, point load
 (d) central crack in shear

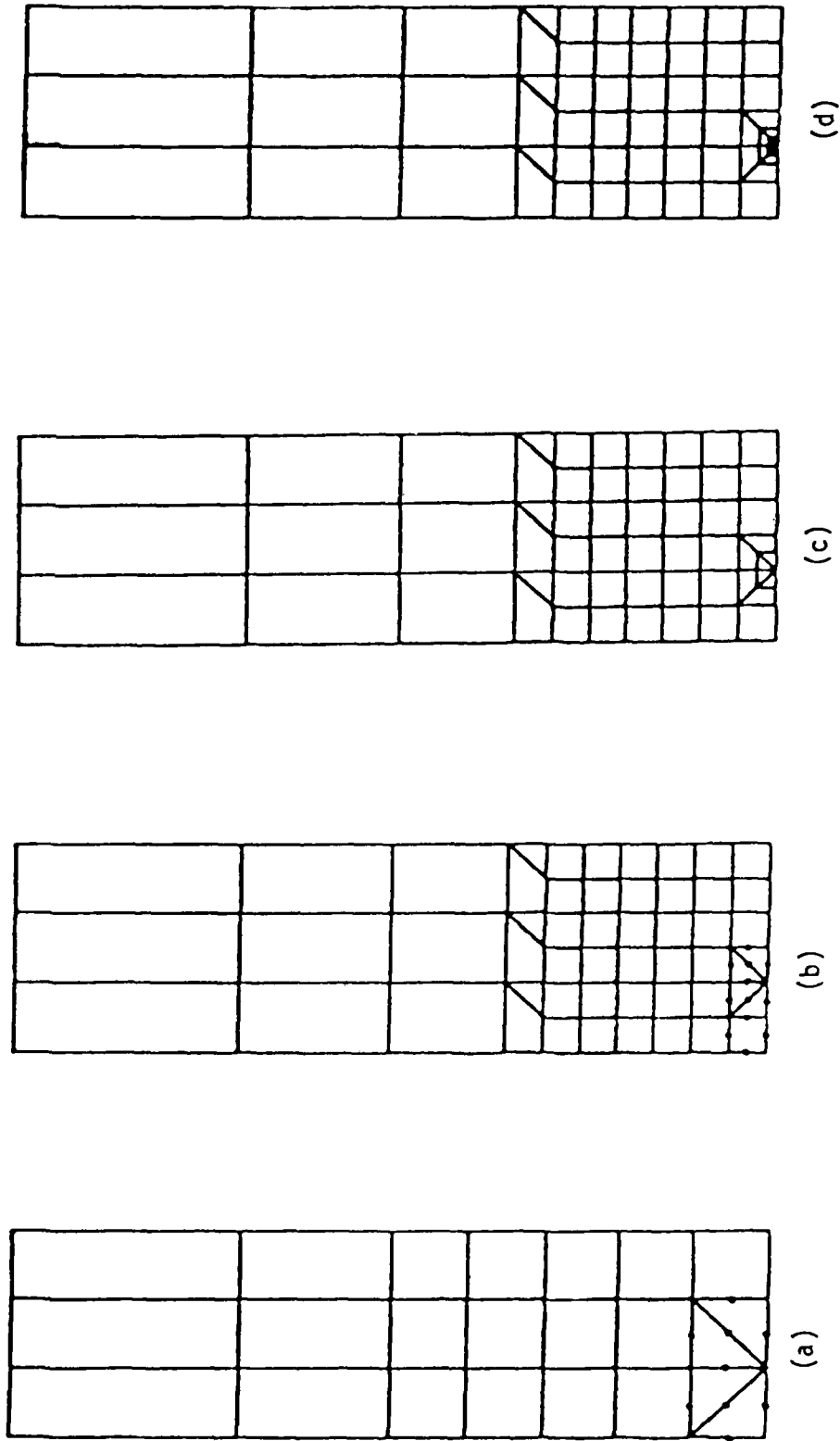


Figure 8 Different mesh sizes analyzed.

- (a) 37 grid mesh
- (b) 77 grid mesh
- (c) 86 grid mesh
- (d) 95 grid mesh

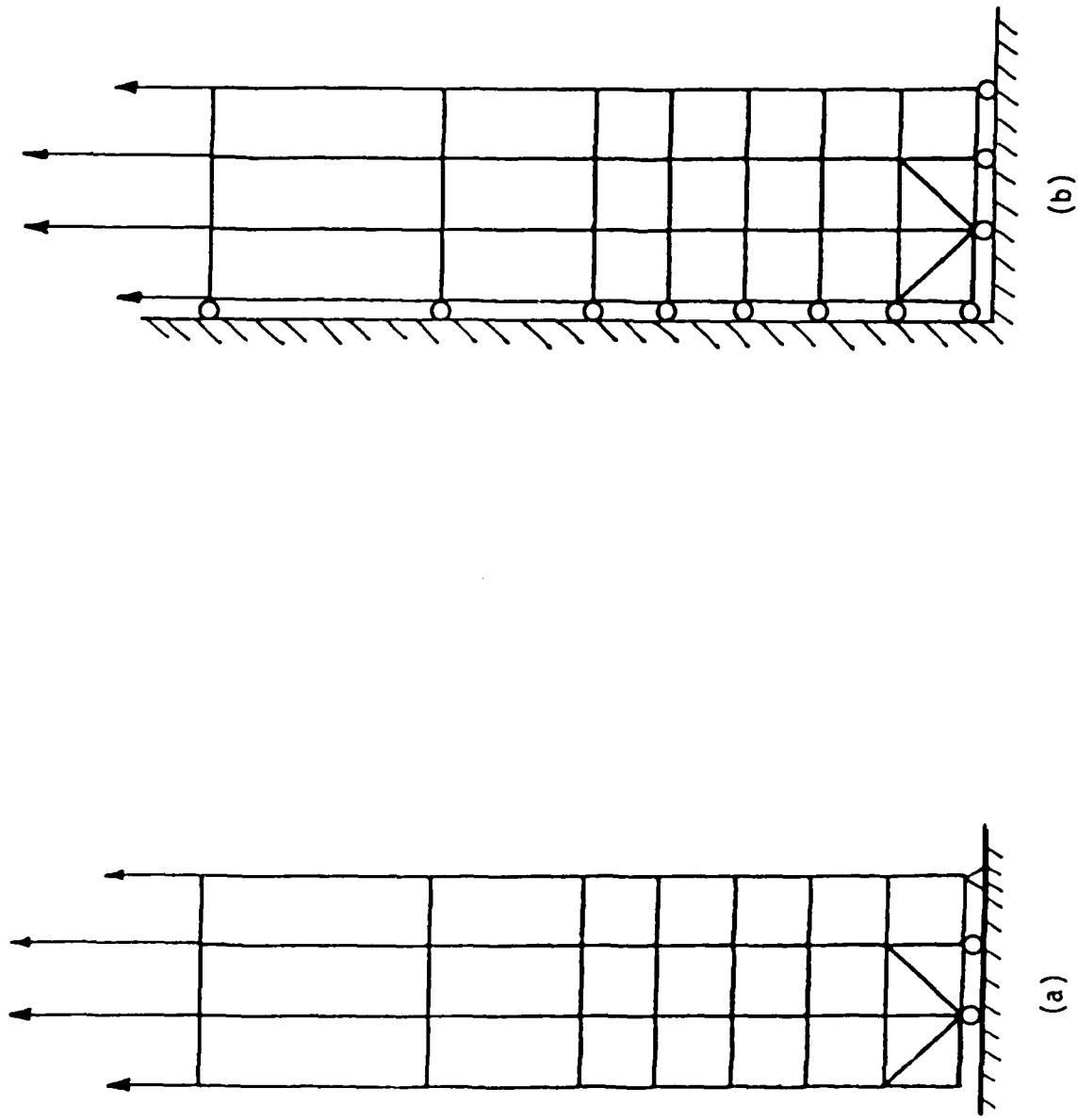


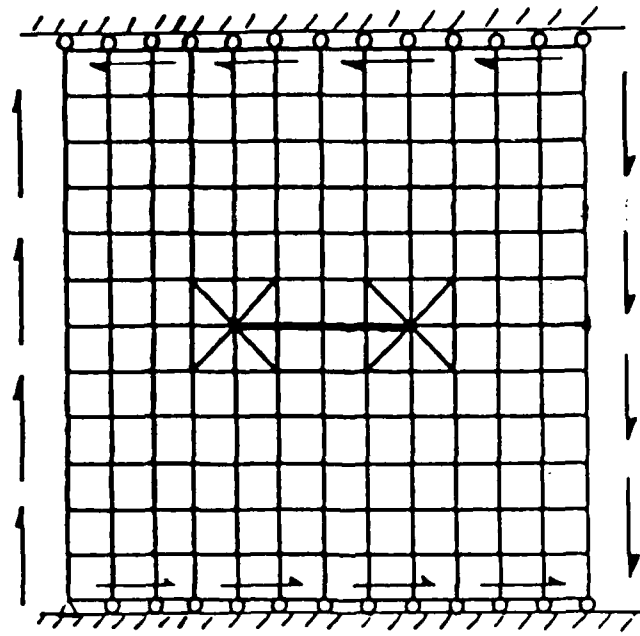
Figure 9 Boundary conditions for edge crack and central crack specimens.
 (a) edge crack
 (b) central crack

TABLE 1 ERRORS IN COD AND K_I AS A FUNCTION OF MESH

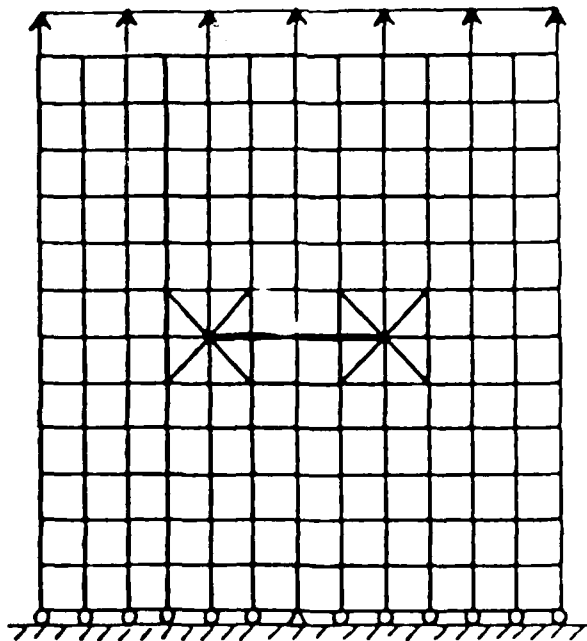
	37 Grid Mesh	77 Grid Mesh	86 Grid Mesh	95 Grid Mesh
CENTRAL CRACK	COD Error (%)	- 7.73	- 2.46	- 2.82
	K_I Error (%)	11.63	2.91	1.69
EDGE CRACK WITH UNIFORM STRESS	COD Error (%)	- 5.24	- 2.51	- 2.60
	K_I Error (%)	- 6.26	- 5.18	- 3.19
EDGE CRACK WITH POINT LOAD	COD Error (%)	-	-	-
	K_I Error (%)	-26.11	- 9.38	- 0.40
				- 2.92
				1.22
				- 2.64
				- 2.05
				-
				5.26

TABLE 2 ERRORS IN K_I AND K_{II} FOR 234 GRID MESH

	Error (%)
CENTRAL CRACK IN SHEAR, FINITE PLATE	K_I
	- 1.37
	K_{II}
	4.23



(a) loading condition for K_{II} calculation



(b) loading condition for K_I calculation

Figure 10 Model of central crack in finite plate.

intensity factor for an edge crack. Another more involved problem which demonstrates calculation of both K_I and K_{II} is also presented.

5.1 REQUIRED USER INPUT AND INTERPRETATION OF OUTPUT

The crack element was implemented using the CDUM1 user element. The formats for the ADUM1, CDUM1, and PDUM1 cards are presented in Figures 11 through 13. The ADUM1 card is used by NASTRAN so that it interprets the associated PDUM1 cards and CDUM1 cards properly. This card should always be used as shown in Figure 11 and only 1 card per NASTRAN bulk data deck is required.

The PDUM1 cards and CDUM1 card fields are described in Figures 12 and 13. Also presented in Figures 12 and 13 are allowable ranges for the various options.

The CDUM1 user output consists of nine headings labeled S1 through S9. Table 3 describes the various output quantities for the crack element. IKI of Table 3 is input on the element's PDUM1 card.

Note that currently, the BANDIT = -1 option must be used on the NASTRAN card.

5.2 SAMPLE PROBLEM FOR CALCULATION OF K_I

Figure 14 presents a crude model for calculating the stress intensity factors for the edge crack with uniform stress. This geometry was previously depicted in Figure 7b, with the associated errors shown in Table 1 under the 37 Grid Mesh column. The bulk data input is shown in Figure 15.

Elements 1 through 4 are singular crack elements while Elements 5, 6, and 9 are non-singular. Note the grid numbering sequence for Elements 1 and 4. Since the stress intensity factors are calculated along rays closest to the element's local x-axis,

BULK DATA DECK

Input Data Card ADUM1

Dummy Element Attributes

Description: Defines attributes of the dummy element CDUM1.

Format and Example:

	1	2	3	4	5	6	7	8	9	10
ADUM1	NG	NC	NP	ND						
ADUM1	8	1	6	3						

Field

- NG Number of grid points connected by DUM1 dummy element
(Integer = 8)
- NC Number of additional entries on CDUM1 connection card
(Integer = 1)
- NP Number of additional entries on PDUM1 property card
(Integer = 6)
- ND Number of displacement components at each grid point
used in generation of differential stiffness matrix
(Integer = 3)

Figure 11 ADUM1 bulk data card for singular or non-singular structural element.

BULK DATA DECK

Input Data Card CDUM1

Dummy Element Connection

Description: Defines a singular or non-singular, two-dimensional structural element. Must be used in conjunction with the Fortran code supplied with this report.

Format and Example:

1	2	3	4	5	6	7	8	9	10
CDUM1	EID	PID	G1	G2	G3	G4	G5	G6	abc
CDUM1	114	108	2	5	6	8	7	11	ABC
+bc	G7	G8							
+BC	12	14							

<u>Field</u>	<u>Contents</u>
EID	Element identification number (Integer > 0)
PID	Identification number of a PDUMI property card (Integer > 0)
G1...G8	Grid point identification numbers of connection points (Integer 0, G1 ≠ G2 ... ≠ G8)
<u>Remarks</u>	<ol style="list-style-type: none"> 1. All grid points must be unique and all eight grids must be present. Dummy grid points must be introduced into the model if the element is to have less than eight grid points. 2. To form a triangle, the x,y,z coordinates of G4 must equal the x,y,z coordinates of G1. G4 is then SPC'd in 123456 and is considered a dummy grid point not used in the analysis. 3. To eliminate any mid-side grid, the x,y,z coordinates of the mid-side grid must equal the x,y,z coordinates of one of the corner grids. The eliminated mid-side grid is then SPC'd in 123456 and is considered a dummy grid point not used in the analysis.

-- continued

Figure 12 CDUM1 bulk data card for singular or non-singular structural element.

CDUM1 (continued)

Remarks

4. Dummy grids may be shared by adjacent elements in order to keep down the total number of required grid points.
5. The ordering convention for the element's grid points G1 through G8 are shown below.

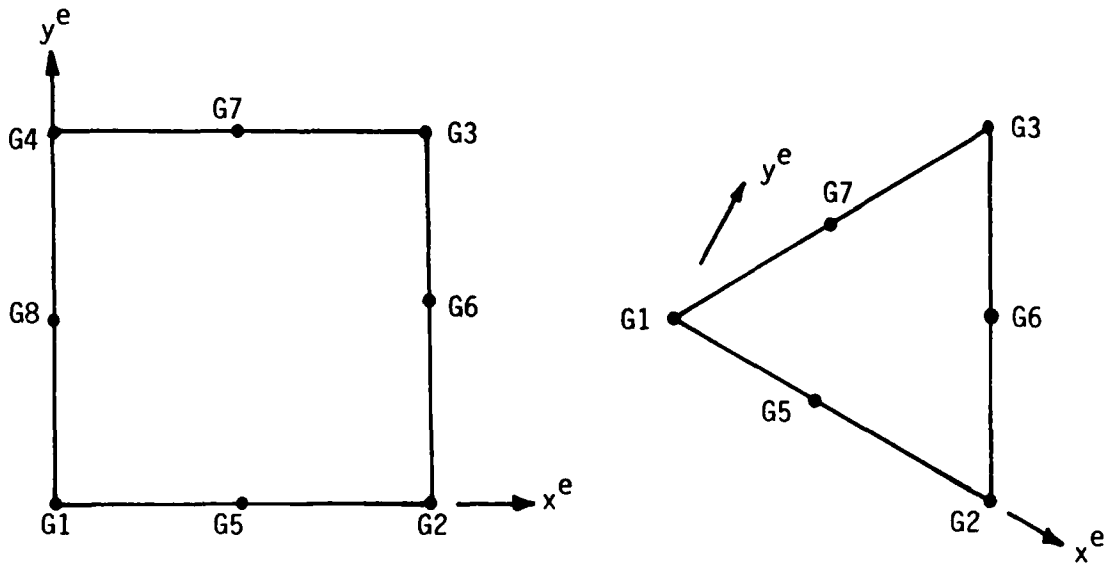


Figure 12 Concluded.

BULK DATA DECK

Input Data Card PDUM1

Dummy Element Property

Description: Defines the properties and stress evaluation techniques to be used with the CDUM1 singular or non-singular element. Must be used in conjunction with the Fortran code supplied with this report.

Format and Example:

1	2	3	4	5	6	7	8	9	10
PDUM1	PID	MID	T	GAMMA	IPLANE	NIPR	NIPS	IKI	
PDUM1	108	2	0.10	0.50	1	5	4	1	

<u>Field</u>	<u>Contents</u>
PID	Property identification number (Integer > 0)
MID	Material identification number (Integer > 0)
T	Element thickness (Real > 0)
GAMMA	Exponent used in displacement field (Real, 0.50 for singular element, 2.0 for non-singular element)
IPLANE	Plane strain or plane stress option, use 0 for plane strain, 1 for plane stress (Integer 0 or 1)
NIPR	Number of integration points in r direction. The r direction is the radial direction for the singular element (0 < Integer < 5)
NIPS	Numer of integration points in s direction (0 < Integer < 5)
IKI	Stress and stress intensity factor calculation option. Use IKI=0 to calculate K_I and K_{II} based upon stresses. Use IKI=1 to calculate K_I and K_{II} based upon displacements. For IKI=2 no stress intensity factor calculations are performed. (Integer 0,1 or 2)

Figure 13 PDUM1 bulk data card for singular or non-singular structural element.

TABLE 3
 INTERPRETATION OF CDUM1 USER ELEMENT STRESS OUTPUT

IKI*	S1	S2	S3	S4	S5	S6	S7	S8	S9
0	x	y	σ_x	σ_y	τ_{xy}	K_I	K_{II}	0	0
1	x	y	σ_x	σ_y	τ_{xy}	K_I	K_{II}	0	0
2	x	y	σ_x	σ_y	τ_{xy}	ϵ_x	ϵ_y	γ_{xy}	0

* For IKI = 0, K_I and K_{II} based on stresses (Equation 8)
 For IKI = 1, K_I and K_{II} based on displacements (Equation 9)
 For IKI = 2, K_I and K_{II} are not calculated

NOTES: x and y are the element coordinates where stresses and strains are reported.


```

NASTRAN BANDIT--1
ID KI TEST
APP DISPLACEMENT
DIAO 8
TIME 15
SOL 1
CEND
TITLE -KITEST.NID - TEST OF CDUM1 ELEMENT, SIDE CRACKED GEOMETRY, 6/10/85
SUBTITLE= EDGE NOTCH, 37 NODES, A/W=1/3, SINGULAR ELE, 5X4 GAUSS
SPC=1
LOAD=1
DISP=ALL
STRESS=ALL
BEGIN BULK
$ 1 .. 2 .. 3 .. 4 .. 5 .. 6 .. 7 .. 8 .. 9 .. 10
$
$ PARAMETERS
$
PARAM GRDPNT 0
PARAM COUPMASS 1
$
$ ***** PDUM1 = 1 SING ELEM W. KI AND KII BASED ON DISPLACEMENTS
$ = 2 NON-SINGULAR ELEM
$ = 3 SING ELEM W. NO KI AND KII CALCS
$ = 4 SING ELEM W. KI AND KII BASED ON STRESSES
$ PQDMEM1 = 3 REGULAR 4 GRID ISOPARAMETRIC ELEM
$
$ MAT1 = 1 MATL PROPS, CDUM1 ADJUSTS THEM FOR PLANE STRAIN
$ MAT1 = 2 MALT PROPS W. E AND NU ADJUSTED FOR PLANE STRAIN
$
ADUM1 8 1 6 3
PDUM1 1 1 1. .5 0 5 4 1
PDUM1 2 1 1. 2. 0 2 2 2
PDUM1 3 1 1. .5 0 5 4 2
PDUM1 4 1 1. .5 0 5 4 0
$
PQDMEM1 3 2 1.
MAT1 1 10.E6 .3 .10
MAT1 2 10.98720 .30572 .10
$
$ ***** SPC=1 IS FOR EDGE CRACK W. UNIFORM TENSION STRESS
$ GRIDS 50-57 ARE DUMMY GRIDS
$
SPC1 1 3456 1 THRU 37
SPC1 1 123456 50 THRU 57
SPC1 1 2 3 4 5 22
SPC1 1 1 22
$
$
FORCE 1 34 0 500. 0. 1.
FORCE 1 35 0 1000. 0. 1.
FORCE 1 36 0 1000. 0. 1.
FORCE 1 37 0 500. 0. 1.
$
$ CDUM1 1-4 ARE CRACK ELEMENTS
$
CDUM1 1 1 3 1 11 50 2 6 +CD1
+CD1 7 51 0.
CDUM1 2 3 3 13 11 50 8 12 +CD2
+CD2 7 51 0.
CDUM1 3 3 3 13 15 50 8 14 +CD3
+CD3 9 51 0.
CDUM1 4 4 3 5 15 50 4 10 +CD4
+CD4 9 51 0.
$
$ ELEM 5,6 AND 9 ARE NONSINGULAR CDUM1 ELEMENTS W MISSING MID-SIDE NODES
$
CDUM1 5 2 11 13 17 16 12 52 +CD5
+CD5 53 54 0.
CDUM1 6 2 13 15 18 17 14 52 +CD6
+CD6 53 54 0.
CDUM1 9 2 5 22 23 15 55 56 +CD9
+CD9 57 10 0.

```

Figure 15 Bulk data for model of Figure 14.

```

$
$   REST ARE CQDMEM1 (4 NODE ISOPARAMETRIC ELEMENTS)
$
CQDMEM1 7      3      16      17      20      19
CQDMEM1 8      3      17      18      21      20
CQDMEM1 10     3      15      23      24      18
CQDMEM1 11     3      18      24      25      21
CQDMEM1 12     3      19      20      27      26
CQDMEM1 13     3      20      21      28      27
CQDMEM1 14     3      21      25      29      28
CQDMEM1 15     3      26      27      31      30
CQDMEM1 17     3      28      29      33      32
CQDMEM1 18     3      30      31      35      34
CQDMEM1 19     3      31      32      36      35
CQDMEM1 20     3      32      33      37      36
$
$
GRID 1      0      0.      0.
GRID 2      0      .5      0.
GRID 3      0      1.      0.
GRID 4      0      1.5     0.
GRID 5      0      2.      0.
GRID 6      0      0.      .5
GRID 7      0      .5      .5
GRID 8      0      1.      .5
GRID 9      0      1.5     .5
GRID 10     0      2.      .5
GRID 11     0      0.      1.
GRID 12     0      .5      1.
GRID 13     0      1.      1.
GRID 14     0      1.5     1.
GRID 15     0      2.      1.
GRID 16     0      0.      2.
GRID 17     0      1.      2.
GRID 18     0      2.      2.
GRID 19     0      0.      3.
GRID 20     0      1.      3.
GRID 21     0      2.      3.
GRID 22     0      3.      0.
GRID 23     0      2.      1.
GRID 24     0      3.      2.
GRID 25     0      3.      3.
GRID 26     0      0.      4.
GRID 27     0      1.      4.
GRID 28     0      2.      4.
GRID 29     0      3.      4.
GRID 30     0      0.      5.
GRID 31     0      1.      5.
GRID 32     0      2.      5.
GRID 33     0      3.      5.
GRID 34     0      0.      7.
GRID 35     0      1.      7.
GRID 36     0      2.      7.
GRID 37     0      3.      7.
$
$   GRIDS 50-57 ARE DUMMY GRIDS FOR CDUM1 ELEMS
$
GRID 50     0      1.      0.
GRID 51     0      1.      0.
GRID 52     0      1.      1.
GRID 53     0      1.      1.
GRID 54     0      1.      1.
GRID 55     0      3.      1.
GRID 56     0      3.      1.
GRID 57     0      3.      1.
ENDDATA

```

Figure 15 Concluded.

Element 1 is numbered as shown. Since the Element 1 x-axis edge forms the cracks surface, the PDUM1 card for Element 1 should request that displacements be used to calculate stress intensity factors. This is consistent with the equations presented in Section 2.3. Element 4 is numbered as shown, and its stress intensity factors are based on stresses. Theoretically, the stress intensity factors predicted for Element 1 and Element 4 should be the same. It has been found that, usually, the displacement-based stress intensity factors are more accurate. For Elements 2 and 3, no stress intensity factor calculations are performed since they would not be meaningful. The numbering for Elements 2 and 3 is not as critical, although the first grid must be located at the crack tip for all singular elements. Since element stresses are in terms of the element's coordinate system, it is suggested that they be aligned with the basic system whenever possible.

Grids 50 and 51 are dummy grids which must be present. Note that they may be shared by any adjacent elements. In order to form a triangular element, the x,y,z coordinates of element grid 4 (G4) must be the same as those of element grid 1 (G1). Mid-side grids are eliminated by making their coordinates equal to that of any of the corner grids. Note also that Elements 5 and 6 share the dummy grids 52, 53, and 54, while Element 9 uses dummy grids 55, 56, and 57.

The theoretical solution for this problem is given in Reference 2, page 2.10 as

$$\begin{aligned}
 K_I &= \sigma \sqrt{\pi a} F\left(\frac{a}{b}\right) \\
 &= 1000 \text{ psi} \sqrt{\pi(1)\text{in}} \times 1.786 \\
 &= 3165 \text{ lb-in}^{-3/2}
 \end{aligned}$$

$$\text{COD} = 2 \times 4.655 \times 10^{-4} \text{ in.}$$

The reported values from the NASTRAN run are:

$$K = 2965 \text{ lb-in}^{-3/2} \quad (\text{Element 1})$$

$$\text{COD} = 2 \times 4.397 \times 10^{-4} \text{ in.} \quad (\text{grid 1})$$

These calculated errors are slightly different than those reported in Table 1. Because the errors reported in Table 1 were calculated using double precision arithmetic, whereas the NASTRAN results shown above use single precision arithmetic for stress recovery.

5.3 SAMPLE PROBLEM FOR CALCULATION OF K_I AND K_{II}

Figure 16 presents the fairly detailed model used to calculate K_I and K_{II} for a central crack in shear. This geometry was previously depicted in Figure 7d, while the loading and boundary conditions are shown in Figure 10. Figure 17 presents the bulk data input for this model. Several additional subcases are also analyzed in the bulk data of Figure 17. The SPC=1 set applies to the shear problem whereas the SPC=2 set is for the tension problem. Other input data are documented in the deck. Figure 16 also shows a blown-up view of the left side of the crack geometry so that it may be easily compared to the bulk data cards. Grids 325 and 326 are the dummy grids for crack Elements 1001 through 1008. The elements used to model the right side of the crack are Elements 2001 through 2008. Other CDUM1 Elements used in the model are transition elements.

The theoretical stress intensity factors, K_{II} , for the shear loading is given in Reference 2, page 10.1, as

$$K_{II} = \tau \sqrt{\pi a} F_A \left(\frac{a}{b} \right)$$

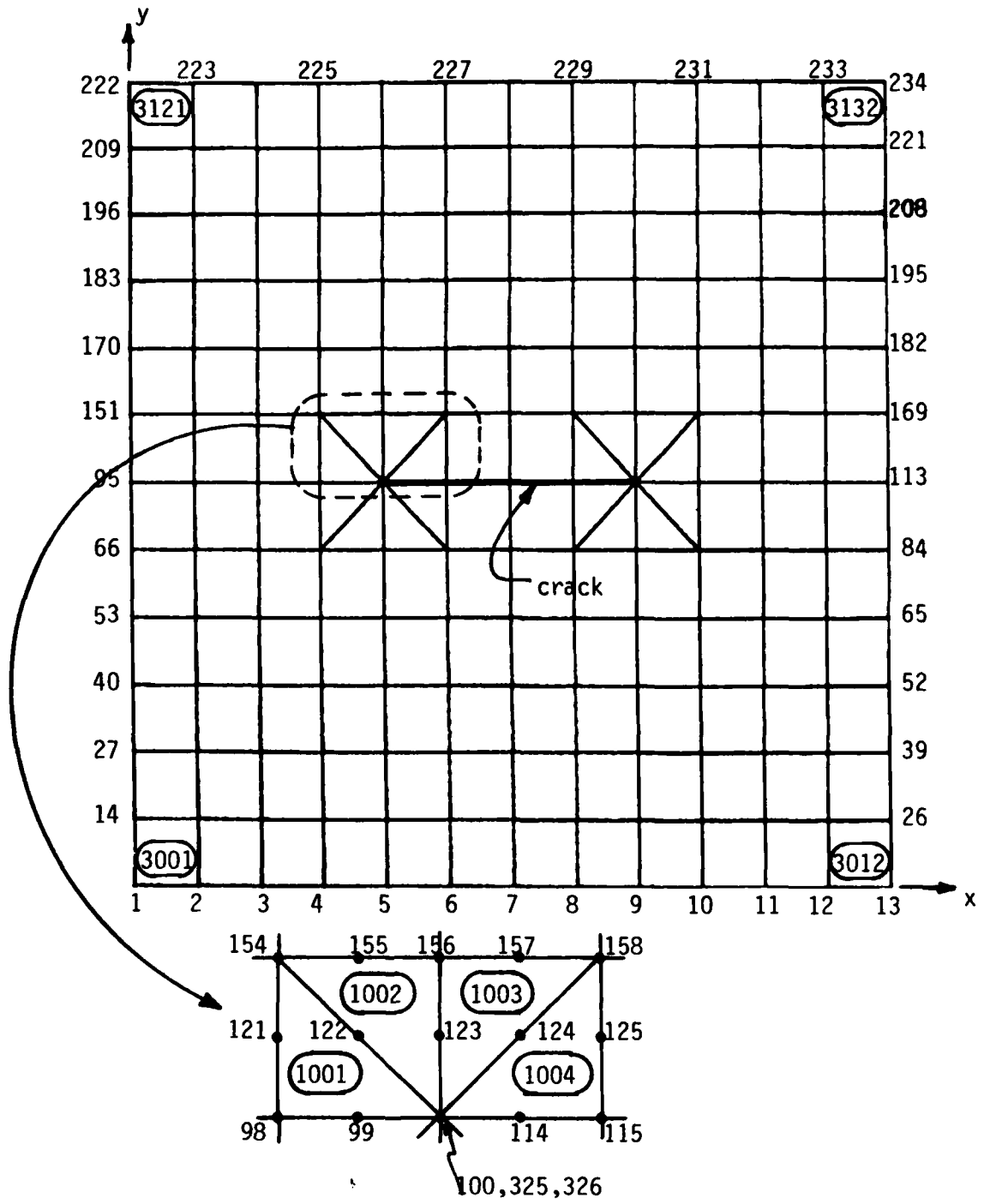


Figure 16 Sample problem for calculation of K_I and K_{II} .

```

NASTRAN BANDIT--1
ID KI TEST
APP DISPLACEMENT
DIAG 8
TIME 15
SOL 1
CEND
TITLE   =K12TEST.NID- KI AND K2 FOR CENTER CRACK, 234 NODES,(A/B=1/3)
SUBTITLE=          SINGULAR ELEMENTS, 5X4 GAUSS
          DISP=ALL
          STRESS=ALL
SUBCASE 1
  LABEL = TENSION LOAD, KI CALCULATION
  SPC =2
  LOAD=2
SUBCASE 2
  LABEL = THERMAL LOAD, UNIFORM TEMPERATURE
  SPC =2
  TEMP(LOAD)=3
SUBCASE 3
  LABEL = COMBINED TENSION + TEMPERATURE
  SPC =2
  LOAD=2
  TEMP(LOAD)=3
$
SUBCASE 4
  LABEL = SHEAR LOAD, KII CALCULATION
  SPC =1
  LOAD=1
SUBCASE 5
  LABEL = THERMAL LOAD W. CONSTRAINED BOUNDARY, INDUCES 10000 PSI TENSION
  SPC=1
  TEMP(LOAD)=4
SUBCASE 6
  LABEL = SHEAR LOAD + THERMAL LOAD, MIXED MODE KI AND KII CALCULATION
  SPC =1
  LOAD=1
  TEMP(LOAD)=4
BEGIN BULK
$ 1 .. 2 .. 3 .. 4 .. 5 .. 6 .. 7 .. 8 .. 9 .. 10
$
$ PARAMETERS
$
PARAM GRDPNT 0
PARAM COUPMASS 1
$
$ ***** PDUM1 = 1 ARE NONSING ELEM
$                = 2 SING ELEM W. ONLY CENTROID STRESS RECOVERY
$                = 3 SING ELEM W. KI AND KII CALCS BASED ON DISPLACEMENTS
$                = 4 SING ELEM W. KI AND KII CALCS BASED ON STRESSES
$                NOTE: ALL OF THESE PDUM1 PROPERTIES ARE FOR PLANE STRAIN
$
$                PQDMEM1 = 1 REGULAR 4 GRID ISOPARAMETRIC ELEMENTS
$
$                MAT1 = 1 MATL PROPS, CDUM1 ADJUSTS THEM FOR PLANE STRAIN
$                MAT1 = 2 MATL PROPS W. E AND NU ADJUSTED FOR PLANE STRAIN
$
ADUM1  8      1      6      3
$
PDUM1  1      1      1.      2.      0      2      2      2
PDUM1  2      1      1.      .5      0      5      4      2
PDUM1  3      1      1.      .5      0      5      4      1
PDUM1  4      1      1.      .5      0      5      4      0
$
$
PQDMEM1 1      2      1.
MAT1  1      10.E6      .3      .10      2.E-5      50.
MAT1  2      10.989E6      .428571      .10      2.E-5      50.

```

Figure 17 Bulk data for model of Figure 16.

```

$
$ ***** SPC-2 IS FOR CENTRAL CRACK IN TENSION, KI CALC *****
$ SPC-1 IS FOR CENTRAL CRACK IN SHEAR, KII CALC
$
$ GRIDS 301-328 DUMMY GRIDS FOR CDUM1 ELEMS
$ GRIDS 133-150 DUMMY GRIDS NOT USED AT ALL
$
SPC1 2 3456 1 THRU 234
SPC1 2 123456 133 THRU 150
SPC1 2 123456 301 THRU 328
$
SPC1 2 1 7
SPC1 2 2 1 THRU 13
$
$
SPC1 1 3456 1 THRU 234
SPC1 1 123456 133 THRU 150
SPC1 1 123456 301 THRU 328
$
SPC1 1 12 1
SPC1 1 2 2 THRU 13
SPC1 1 2 222 THRU 234
$
$ ***** SID=3 IS UNIFORM TEMP OF 100, (INDUCES 0 STRESS W. SPC-2)
$ -4 IS UNIFORM TEMP OF 0, (INDUCES 10000 PSI TENSION W. SPC-1)
$
TEMPD 3 100.
TEMPD 4 0.
$
$ ***** LID-2 IS FOR CENTRAL CRACK IN TENSION, KI CALC *****
$ -1 IS FOR CENTRAL CRACK IN SHEAR, KII CALC
$
FORCE 2 222 0 250. 0. 1.
FORCE 2 223 0 500. 0. 1.
FORCE 2 224 0 500. 0. 1.
FORCE 2 225 0 500. 0. 1.
FORCE 2 226 0 500. 0. 1.
FORCE 2 227 0 500. 0. 1.
FORCE 2 228 0 500. 0. 1.
FORCE 2 229 0 500. 0. 1.
FORCE 2 230 0 500. 0. 1.
FORCE 2 231 0 500. 0. 1.
FORCE 2 232 0 500. 0. 1.
FORCE 2 233 0 500. 0. 1.
FORCE 2 234 0 250. 0. 1.
$
FORCE 1 2 0 500. 1. 0.
FORCE 1 3 0 500. 1. 0.
FORCE 1 4 0 500. 1. 0.
FORCE 1 5 0 500. 1. 0.
FORCE 1 6 0 500. 1. 0.
FORCE 1 7 0 500. 1. 0.
FORCE 1 8 0 500. 1. 0.
FORCE 1 9 0 500. 1. 0.
FORCE 1 10 0 500. 1. 0.
FORCE 1 11 0 500. 1. 0.
FORCE 1 12 0 500. 1. 0.
FORCE 1 13 0 250. 1. 0.
$
FORCE 1 14 0 500. 0. 1.
FORCE 1 26 0 -500. 0. 1.
FORCE 1 27 0 500. 0. 1.
FORCE 1 39 0 -500. 0. 1.
FORCE 1 40 0 500. 0. 1.
FORCE 1 52 0 -500. 0. 1.
FORCE 1 57 0 500. 0. 1.
FORCE 1 65 0 -500. 0. 1.
FORCE 1 66 0 500. 0. 1.
FORCE 1 84 0 -500. 0. 1.
FORCE 1 95 0 500. 0. 1.

```

Figure 17 Continued.

FORCE	1	113	0	-500.	0.	1.
FORCE	1	151	0	500.	0.	1.
FORCE	1	169	0	-500.	0.	1.
FORCE	1	170	0	500.	0.	1.
FORCE	1	182	0	-500.	0.	1.
FORCE	1	183	0	500.	0.	1.
FORCE	1	195	0	-500.	0.	1.
FORCE	1	196	0	500.	0.	1.
FORCE	1	208	0	-500.	0.	1.
FORCE	1	209	0	500.	0.	1.
FORCE	1	221	0	-500.	0.	1.
\$						
FORCE	1	222	0	-250.	1.	0.
FORCE	1	223	0	-500.	1.	0.
FORCE	1	224	0	-500.	1.	0.
FORCE	1	225	0	-500.	1.	0.
FORCE	1	226	0	-500.	1.	0.
FORCE	1	227	0	-500.	1.	0.
FORCE	1	228	0	-500.	1.	0.
FORCE	1	229	0	-500.	1.	0.
FORCE	1	230	0	-500.	1.	0.
FORCE	1	231	0	-500.	1.	0.
FORCE	1	232	0	-500.	1.	0.
FORCE	1	233	0	-500.	1.	0.
FORCE	1	234	0	-250.	1.	0.
\$						
\$ GEOMETRY						
\$						
GRID		1	0	0.000	0.000	
GRID		2	0	0.500	0.000	
GRID		3	0	1.000	0.000	
GRID		4	0	1.500	0.000	
GRID		5	0	2.000	0.000	
GRID		6	0	2.500	0.000	
GRID		7	0	3.000	0.000	
GRID		8	0	3.500	0.000	
GRID		9	0	4.000	0.000	
GRID		10	0	4.500	0.000	
GRID		11	0	5.000	0.000	
GRID		12	0	5.500	0.000	
GRID		13	0	6.000	0.000	
GRID		14	0	0.000	0.500	
GRID		15	0	0.500	0.500	
GRID		16	0	1.000	0.500	
GRID		17	0	1.500	0.500	
GRID		18	0	2.000	0.500	
GRID		19	0	2.500	0.500	
GRID		20	0	3.000	0.500	
GRID		21	0	3.500	0.500	
GRID		22	0	4.000	0.500	
GRID		23	0	4.500	0.500	
GRID		24	0	5.000	0.500	
GRID		25	0	5.500	0.500	
GRID		26	0	6.000	0.500	
GRID		27	0	0.000	1.000	
GRID		28	0	0.500	1.000	
GRID		29	0	1.000	1.000	
GRID		30	0	1.500	1.000	
GRID		31	0	2.000	1.000	
GRID		32	0	2.500	1.000	
GRID		33	0	3.000	1.000	
GRID		34	0	3.500	1.000	
GRID		35	0	4.000	1.000	
GRID		36	0	4.500	1.000	
GRID		37	0	5.000	1.000	
GRID		38	0	5.500	1.000	
GRID		39	0	6.000	1.000	
GRID		40	0	0.000	1.500	
GRID		41	0	0.500	1.500	
GRID		42	0	1.000	1.500	
GRID		43	0	1.500	1.500	
GRID		44	0	2.000	1.500	
GRID		45	0	2.500	1.500	
GRID		46	0	3.000	1.500	
GRID		47	0	3.500	1.500	

Figure 17 Continued.

GRID	48	0	4.000	1.500
GRID	49	0	4.500	1.500
GRID	50	0	5.000	1.500
GRID	51	0	5.500	1.500
GRID	52	0	6.000	1.500
GRID	53	0	0.000	2.000
GRID	54	0	0.500	2.000
GRID	55	0	1.000	2.000
GRID	56	0	1.500	2.000
GRID	57	0	2.000	2.000
GRID	58	0	2.500	2.000
GRID	59	0	3.000	2.000
GRID	60	0	3.500	2.000
GRID	61	0	4.000	2.000
GRID	62	0	4.500	2.000
GRID	63	0	5.000	2.000
GRID	64	0	5.500	2.000
GRID	65	0	6.000	2.000
GRID	66	0	0.000	2.500
GRID	67	0	0.500	2.500
GRID	68	0	1.000	2.500
GRID	69	0	1.500	2.500
GRID	70	0	1.750	2.500
GRID	71	0	2.000	2.500
GRID	72	0	2.250	2.500
GRID	73	0	2.500	2.500
GRID	74	0	2.750	2.500
GRID	75	0	3.000	2.500
GRID	76	0	3.250	2.500
GRID	77	0	3.500	2.500
GRID	78	0	3.750	2.500
GRID	79	0	4.000	2.500
GRID	80	0	4.250	2.500
GRID	81	0	4.500	2.500
GRID	82	0	5.000	2.500
GRID	83	0	5.500	2.500
GRID	84	0	6.000	2.500
GRID	85	0	1.500	2.750
GRID	86	0	1.750	2.750
GRID	87	0	2.000	2.750
GRID	88	0	2.250	2.750
GRID	89	0	2.500	2.750
GRID	90	0	3.000	2.750
GRID	91	0	3.500	2.750
GRID	92	0	3.750	2.750
GRID	93	0	4.000	2.750
GRID	94	0	4.250	2.750
GRID	95	0	0.000	3.000
GRID	96	0	0.500	3.000
GRID	97	0	1.000	3.000
GRID	98	0	1.500	3.000
GRID	99	0	1.750	3.000
GRID	100	0	2.000	3.000
GRID	101	0	2.250	3.000
GRID	102	0	2.500	3.000
GRID	103	0	2.750	3.000
GRID	104	0	3.000	3.000
GRID	105	0	3.250	3.000
GRID	106	0	3.500	3.000
GRID	107	0	3.750	3.000
GRID	108	0	4.000	3.000
GRID	109	0	4.250	3.000
GRID	110	0	4.500	3.000
GRID	111	0	5.000	3.000
GRID	112	0	5.500	3.000
GRID	113	0	6.000	3.000
GRID	114	0	2.250	3.000
GRID	115	0	2.500	3.000
GRID	116	0	2.750	3.000
GRID	117	0	3.000	3.000
GRID	118	0	3.250	3.000
GRID	119	0	3.500	3.000
GRID	120	0	3.750	3.000
GRID	121	0	1.500	3.250
GRID	122	0	1.750	3.250

Figure 17 - Continued.

GRID	123	0	2.000	3.250
GRID	124	0	2.250	3.250
GRID	125	0	2.500	3.250
GRID	126	0	3.000	3.250
GRID	127	0	3.500	3.250
GRID	128	0	3.750	3.250
GRID	129	0	4.000	3.250
GRID	130	0	4.250	3.250
GRID	131	0	4.500	3.250
GRID	132	0	4.500	2.750
GRID	133	0	0.000	0.000
GRID	134	0	0.000	0.000
GRID	135	0	0.000	0.000
GRID	136	0	0.000	0.000
GRID	137	0	0.000	0.000
GRID	138	0	0.000	0.000
GRID	139	0	0.000	0.000
GRID	140	0	0.000	0.000
GRID	141	0	0.000	0.000
GRID	142	0	0.000	0.000
GRID	143	0	0.000	0.000
GRID	144	0	0.000	0.000
GRID	145	0	0.000	0.000
GRID	146	0	0.000	0.000
GRID	147	0	0.000	0.000
GRID	148	0	0.000	0.000
GRID	149	0	0.000	0.000
GRID	150	0	0.000	0.000
GRID	151	0	0.000	3.500
GRID	152	0	0.500	3.500
GRID	153	0	1.000	3.500
GRID	154	0	1.500	3.500
GRID	155	0	1.750	3.500
GRID	156	0	2.000	3.500
GRID	157	0	2.250	3.500
GRID	158	0	2.500	3.500
GRID	159	0	2.750	3.500
GRID	160	0	3.000	3.500
GRID	161	0	3.250	3.500
GRID	162	0	3.500	3.500
GRID	163	0	3.750	3.500
GRID	164	0	4.000	3.500
GRID	165	0	4.250	3.500
GRID	166	0	4.500	3.500
GRID	167	0	5.000	3.500
GRID	168	0	5.500	3.500
GRID	169	0	6.000	3.500
GRID	170	0	0.000	4.000
GRID	171	0	0.500	4.000
GRID	172	0	1.000	4.000
GRID	173	0	1.500	4.000
GRID	174	0	2.000	4.000
GRID	175	0	2.500	4.000
GRID	176	0	3.000	4.000
GRID	177	0	3.500	4.000
GRID	178	0	4.000	4.000
GRID	179	0	4.500	4.000
GRID	180	0	5.000	4.000
GRID	181	0	5.500	4.000
GRID	182	0	6.000	4.000
GRID	183	0	0.000	4.500
GRID	184	0	0.500	4.500
GRID	185	0	1.000	4.500
GRID	186	0	1.500	4.500
GRID	187	0	2.000	4.500
GRID	188	0	2.500	4.500
GRID	189	0	3.000	4.500
GRID	190	0	3.500	4.500
GRID	191	0	4.000	4.500
GRID	192	0	4.500	4.500
GRID	193	0	5.000	4.500
GRID	194	0	5.500	4.500
GRID	195	0	6.000	4.500
GRID	196	0	0.000	5.000
GRID	197	0	0.500	5.000

Figure 17 Continued.

GRID	198	0	1.000	5.000
GRID	199	0	1.500	5.000
GRID	200	0	2.000	5.000
GRID	201	0	2.500	5.000
GRID	202	0	3.000	5.000
GRID	203	0	3.500	5.000
GRID	204	0	4.000	5.000
GRID	205	0	4.500	5.000
GRID	206	0	5.000	5.000
GRID	207	0	5.500	5.000
GRID	208	0	6.000	5.000
GRID	209	0	0.000	5.500
GRID	210	0	0.500	5.500
GRID	211	0	1.000	5.500
GRID	212	0	1.500	5.500
GRID	213	0	2.000	5.500
GRID	214	0	2.500	5.500
GRID	215	0	3.000	5.500
GRID	216	0	3.500	5.500
GRID	217	0	4.000	5.500
GRID	218	0	4.500	5.500
GRID	219	0	5.000	5.500
GRID	220	0	5.500	5.500
GRID	221	0	6.000	5.500
GRID	222	0	0.000	6.000
GRID	223	0	0.500	6.000
GRID	224	0	1.000	6.000
GRID	225	0	1.500	6.000
GRID	226	0	2.000	6.000
GRID	227	0	2.500	6.000
GRID	228	0	3.000	6.000
GRID	229	0	3.500	6.000
GRID	230	0	4.000	6.000
GRID	231	0	4.500	6.000
GRID	232	0	5.000	6.000
GRID	233	0	5.500	6.000
GRID	234	0	6.000	6.000
\$ DUMMY GRIDS FOR CDUM1 ELEMENTS				
\$GRID	57	0	2.000	2.000
GRID	301	0	2.000	2.000
GRID	302	0	2.000	2.000
GRID	303	0	2.000	2.000
\$				
\$GRID	59	0	3.000	2.000
GRID	304	0	3.000	2.000
GRID	305	0	3.000	2.000
GRID	306	0	3.000	2.000
\$				
\$GRID	61	0	4.000	2.000
GRID	307	0	4.000	2.000
GRID	308	0	4.000	2.000
GRID	309	0	4.000	2.000
\$				
\$GRID	111	0	5.000	3.000
GRID	310	0	5.000	3.000
GRID	311	0	5.000	3.000
GRID	312	0	5.000	3.000
\$				
\$GRID	178	0	4.000	4.000
GRID	313	0	4.000	4.000
GRID	314	0	4.000	4.000
GRID	315	0	4.000	4.000
\$				
\$GRID	176	0	3.000	4.000
GRID	316	0	3.000	4.000
GRID	317	0	3.000	4.000
GRID	318	0	3.000	4.000
\$				
\$GRID	174	0	2.000	4.000
GRID	319	0	2.000	4.000
GRID	320	0	2.000	4.000
GRID	321	0	2.000	4.000

Figure 17 Continued.

\$									
\$GRID	97	0	1.000	3.000					
GRID	322	0	1.000	3.000					
GRID	323	0	1.000	3.000					
GRID	324	0	1.000	3.000					
\$									
\$GRID	100	0	2.000	3.000					
GRID	325	0	2.000	3.000					
GRID	326	0	2.000	3.000					
\$									
\$GRID	108	0	4.000	3.000					
GRID	327	0	4.000	3.000					
GRID	328	0	4.000	3.000					
\$									
\$									
CDUM1	1001	4	100	98	154	325	99	121+CD	1001
+CD 1001	122	326							
CDUM1	1002	2	100	156	154	325	123	155+CD	1002
+CD 1002	122	326							
CDUM1	1003	2	100	156	158	325	123	157+CD	1003
+CD 1003	124	326							
CDUM1	1004	3	100	115	158	325	114	125+CD	1004
+CD 1004	124	326							
CDUM1	1005	3	100	102	73	325	101	89+CD	1005
+CD 1005	88	326							
CDUM1	1006	2	100	71	73	325	87	72+CD	1006
+CD 1006	88	326							
CDUM1	1007	2	100	71	69	325	87	70+CD	1007
+CD 1007	86	326							
CDUM1	1008	4	100	98	69	325	99	85+CD	1008
+CD 1008	86	326							
\$									
CDUM1	2001	3	108	119	162	327	120	127+CD	2001
+CD 2001	128	328							
CDUM1	2002	2	108	164	162	327	129	163+CD	2002
+CD 2002	128	328							
CDUM1	2003	2	108	164	166	327	129	165+CD	2003
+CD 2003	130	328							
CDUM1	2004	4	108	110	166	327	109	131+CD	2004
+CD 2004	130	328							
CDUM1	2005	4	108	110	81	327	109	132+CD	2005
+CD 2005	94	328							
CDUM1	2006	2	108	79	81	327	93	80+CD	2006
+CD 2006	94	328							
CDUM1	2007	2	108	79	77	327	93	78+CD	2007
+CD 2007	92	328							
CDUM1	2008	3	108	106	77	327	107	91+CD	2008
+CD 2008	92	328							
\$									
CQDMEM1	3001	1	1	2	15	14			
CQDMEM1	3002	1	2	3	16	15			
CQDMEM1	3003	1	3	4	17	16			
CQDMEM1	3004	1	4	5	18	17			
CQDMEM1	3005	1	5	6	19	18			
CQDMEM1	3006	1	6	7	20	19			
CQDMEM1	3007	1	7	8	21	20			
CQDMEM1	3008	1	8	9	22	21			
CQDMEM1	3009	1	9	10	23	22			
CQDMEM1	3010	1	10	11	24	23			
CQDMEM1	3011	1	11	12	25	24			
CQDMEM1	3012	1	12	13	26	25			
CQDMEM1	3013	1	14	15	28	27			
CQDMEM1	3014	1	15	16	29	28			
CQDMEM1	3015	1	16	17	30	29			
CQDMEM1	3016	1	17	18	31	30			
CQDMEM1	3017	1	18	19	32	31			
CQDMEM1	3018	1	19	20	33	32			
CQDMEM1	3019	1	20	21	34	33			
CQDMEM1	3020	1	21	22	35	34			
CQDMEM1	3021	1	22	23	36	35			
CQDMEM1	3022	1	23	24	37	36			
CQDMEM1	3023	1	24	25	38	37			
CQDMEM1	3024	1	25	26	39	38			

Figure 17 Continued.

CQDMEM1	3025	1	27	28	41	40		
CQDMEM1	3026	1	28	29	42	41		
CQDMEM1	3027	1	29	30	43	42		
CQDMEM1	3028	1	30	31	44	43		
CQDMEM1	3029	1	31	32	45	44		
CQDMEM1	3030	1	32	33	46	45		
CQDMEM1	3031	1	33	34	47	46		
CQDMEM1	3032	1	34	35	48	47		
CQDMEM1	3033	1	35	36	49	48		
CQDMEM1	3034	1	36	37	50	49		
CQDMEM1	3035	1	37	38	51	50		
CQDMEM1	3036	1	38	39	52	51		
CQDMEM1	3037	1	40	41	54	53		
CQDMEM1	3038	1	41	42	55	54		
CQDMEM1	3039	1	42	43	56	55		
CQDMEM1	3040	1	43	44	57	56		
CQDMEM1	3041	1	44	45	58	57		
CQDMEM1	3042	1	45	46	59	58		
CQDMEM1	3043	1	46	47	60	59		
CQDMEM1	3044	1	47	48	61	60		
CQDMEM1	3045	1	48	49	62	61		
CQDMEM1	3046	1	49	50	63	62		
CQDMEM1	3047	1	50	51	64	63		
CQDMEM1	3048	1	51	52	65	64		
CQDMEM1	3049	1	53	54	67	66		
CQDMEM1	3050	1	54	55	69	67		
CQDMEM1	3051	1	55	56	69	68		
CDUM1	3052	1	56	57	71	69	301	302+CD 3052
+CD 3052	70	303						
CDUM1	3053	1	57	58	73	71	301	302+CD 3053
+CD 3053	72	303						
CDUM1	3054	1	58	59	75	73	304	305+CD 3054
+CD 3054	74	306						
CDUM1	3055	1	59	60	77	75	304	305+CD 3055
+CD 3055	76	306						
CDUM1	3056	1	60	61	79	77	307	308+CD 3056
+CD 3056	78	309						
CDUM1	3057	1	61	62	81	79	307	308+CD 3057
+CD 3057	80	309						
CQDMEM1	3058	1	62	63	82	81		
CQDMEM1	3059	1	63	64	83	82		
CQDMEM1	3060	1	64	65	84	83		
CQDMEM1	3061	1	66	67	96	95		
CQDMEM1	3062	1	67	68	97	96		
CDUM1	3063	1	68	69	98	97	322	85+CD 3063
+CD 3063	323	324						
CDUM1	3064	1	81	82	111	110	310	311+CD 3064
+CD 3064	312	132						
CQDMEM1	3065	1	82	83	112	111		
CQDMEM1	3066	1	83	84	113	112		
CQDMEM1	3067	1	95	96	152	151		
CQDMEM1	3068	1	96	97	153	152		
CDUM1	3069	1	97	98	154	153	322	121+CD 3069
+CD 3069	323	324						
CDUM1	3070	1	110	111	167	166	310	311+CD 3070
+CD 3070	312	131						
CQDMEM1	3071	1	111	112	168	167		
CQDMEM1	3072	1	112	113	169	168		
CQDMEM1	3073	1	151	152	171	170		
CQDMEM1	3074	1	152	153	172	171		
CQDMEM1	3075	1	153	154	173	172		
CDUM1	3076	1	154	156	174	173	155	319+CD 3076
+CD 3076	320	321						
CDUM1	3077	1	156	158	175	174	157	319+CD 3077
+CD 3077	320	321						
CDUM1	3078	1	158	160	176	175	159	316+CD 3078
+CD 3078	317	318						
CDUM1	3079	1	160	162	177	176	161	316+CD 3079
+CD 3079	317	318						
CDUM1	3080	1	162	164	178	177	163	313+CD 3080
+CD 3080	314	315						
CDUM1	3081	1	164	166	179	178	165	313+CD 3081
+CD 3081	314	315						

Figure 17 Continued.

CQDMEM1	3082	1	166	167	180	179		
CQDMEM1	3083	1	167	168	181	180		
CQDMEM1	3084	1	168	169	182	181		
CQDMEM1	3085	1	170	171	184	183		
CQDMEM1	3086	1	171	172	185	184		
CQDMEM1	3087	1	172	173	186	185		
CQDMEM1	3088	1	173	174	187	186		
CQDMEM1	3089	1	174	175	188	187		
CQDMEM1	3090	1	175	176	189	188		
CQDMEM1	3091	1	176	177	190	189		
CQDMEM1	3092	1	177	178	191	190		
CQDMEM1	3093	1	178	179	192	191		
CQDMEM1	3094	1	179	180	193	192		
CQDMEM1	3095	1	180	181	194	193		
CQDMEM1	3096	1	181	182	195	194		
CQDMEM1	3097	1	183	184	197	196		
CQDMEM1	3098	1	184	185	198	197		
CQDMEM1	3099	1	185	186	199	198		
CQDMEM1	3100	1	186	187	200	199		
CQDMEM1	3101	1	187	188	201	200		
CQDMEM1	3102	1	188	189	202	201		
CQDMEM1	3103	1	189	190	203	202		
CQDMEM1	3104	1	190	191	204	203		
CQDMEM1	3105	1	191	192	205	204		
CQDMEM1	3106	1	192	193	206	205		
CQDMEM1	3107	1	193	194	207	206		
CQDMEM1	3108	1	194	195	208	207		
CQDMEM1	3109	1	196	197	210	209		
CQDMEM1	3110	1	197	198	211	210		
CQDMEM1	3111	1	198	199	212	211		
CQDMEM1	3112	1	199	200	213	212		
CQDMEM1	3113	1	200	201	214	213		
CQDMEM1	3114	1	201	202	215	214		
CQDMEM1	3115	1	202	203	216	215		
CQDMEM1	3116	1	203	204	217	216		
CQDMEM1	3117	1	204	205	218	217		
CQDMEM1	3118	1	205	206	219	218		
CQDMEM1	3119	1	206	207	220	219		
CQDMEM1	3120	1	207	208	221	220		
CQDMEM1	3121	1	209	210	223	222		
CQDMEM1	3122	1	210	211	224	223		
CQDMEM1	3123	1	211	212	225	224		
CQDMEM1	3124	1	212	213	226	225		
CQDMEM1	3125	1	213	214	227	226		
CQDMEM1	3126	1	214	215	228	227		
CQDMEM1	3127	1	215	216	229	228		
CQDMEM1	3128	1	216	217	230	229		
CQDMEM1	3129	1	217	218	231	230		
CQDMEM1	3130	1	218	219	232	231		
CQDMEM1	3131	1	219	220	233	232		
CQDMEM1	3132	1	220	221	234	233		
CDUM1	3133	1	73	75	104	102	74	90+CD 3133
+CD 3133	103	89						
CDUM1	3134	1	75	77	106	104	76	91+CD 3134
+CD 3134	105	90						
CDUM1	3135	1	115	117	160	158	116	126+CD 3135
+CD 3135	159	125						
CDUM1	3136	1	117	119	162	160	118	127+CD 3136
+CD 3136	161	126						
\$								
ENDDATA								

Figure 17 Concluded.

$$K_{II} = 1000 \text{ psi } \sqrt{\pi(1)in} \times 1.04 = 1843 \text{ lb-in}^{-3/2}$$

while the crack opening displacement (COD) is not reported.

The corresponding K_{II} as reported by NASTRAN is:

$$K_{II} = 1924 \text{ lb-in}^{-3/2} \quad (\text{Subcase 4, Element 1004})$$

Again, a slight discrepancy exists between these results and those reported in Table 2 due to the single versus double precision method of stress calculations previously described.

6.0 SUMMARY AND CONCLUSIONS

The theory, implementation, and user instructions for a linear elastic, two-dimensional COSMIC/NASTRAN crack tip element have been presented. The element was incorporated using the dummy element capability of NASTRAN. Subroutines for calculating the stiffness matrix, mass matrix, thermal load vector, stresses, and stress intensity factors have been developed. Instructions for using the element along with sample problems have been presented.

The stress intensities and crack opening displacements obtained using the element have been compared to several theoretical solutions. Both COD and stress intensity factors appear to be accurately represented even for relatively coarse meshes. The accuracies obtained are well within the accuracies required by typical engineering calculations, since the scatter alone, in the K_I values from a typical test may be 10%.

Finally, due to the generality of the element, extensions to include anisotropic materials and plasticity should be easily accommodated. The work performed here provides a solid theoretical and implementational basis for developing an enhanced version of this element.

REFERENCES

1. Rolfe, S. T. and Barsom, J. M., Fracture and Fatigue Control in Structures, Prentice-Hall, New Jersey, 1977.
2. Tada, H., Paris, P. C., and Irwin, G. R., The Stress Analysis of Cracks Handbook, Del Research Corporation, Hellertown, Penn., 1973.
3. Barsom, R. S., "On the Use of Isoparametric Finite Elements in Linear Fracture Mechanics," International Journal for Numerical Methods in Engineering, Vol. 10, pp. 25-37, 1976.
4. Griffith, A. A., "The Phenomena of Rupture and Flow in Solids," Philosophical Transactions, Royal Soc. (London), Series A., Vol. 221, pp. 163-198, 1920.
5. Erdogan, F., "Stress Intensity Factors," Journal of Applied Mechanics, Vol. 50, pp. 992-1002, 1983.
6. Westergaard, H. M., "Bearing Pressures and Cracks," Journal of Applied Mechanics, Vol. 61, pp. A49-53, 1939.
7. Sneddon, I. N., "The Distribution of Stress in the Neighborhood of a Crack in an Elastic Solid," Proc. Royal Society London, Series A, Vol. 187, pp. 229-260, 1946.
8. Irwin, G. R., "Fracture Mechanics," Structural Mechanics, Goodier and Hoff, eds., Pergamon Press, NY, pp. 557-591, 1960.
9. Wu, E. M., "Application of Fracture Mechanics to Anisotropic Plates," Trans. ASME, Journal of Applied Mechanics, Vol. 34, pp. 967-974, 1967.
10. Broek, D., Elementary Engineering Fracture Mechanics, Noordhoff, Leiden, Third Edition, pp. 359-365, 1983.
11. Erdogan, F. and Sih, G. C., "On Crack Extension in Plates Under Plane Loading and Transverse Shear," Trans. ASME, J. Bas. Engng., - Vol. 85, pp. 519-527, 1963.
12. Sih, G. C., Editor, Mechanics of Fracture, Vol. I, Noordhoff, Leyden, 1973.
13. Henshell, R. D. and Shaw, K. G., "Crack Tip Finite Elements are Unnecessary," International Journal for Numerical Methods in Engineering, Vol. 9, pp. 495-507, 1975.

REFERENCES (Continued)

14. Stern, M., "Families of Consistent Conforming Elements with Singular Derivatives Fields," International Journal for Numerical Methods in Engineering, Vol. 14, pp. 409-421, 1979.
15. Hughes, T. J. R. and Akin, J. E., "Techniques for Developing Special Finite Element Shape Functions with Particular Reference to Singularities," International Journal for Numerical Methods in Engineering, Vol. 15, pp. 733-751, 1980.
16. Bathe, K. J. and Wilson, E. L., Numerical Methods in Finite Element Analysis, Prentice-Hall, 1976.
17. Zienkiewicz, O. C., The Finite Element Method, McGraw-Hill, 1977.
18. The "NASTRAN Programmer's Manual," NASA SP-223(03), July 1976.

APPENDIX

MAGNETIC TAPE FORMAT AND PROCEDURE FOR INSTALLATION OF DUMMY ELEMENT CODE ON VAX COMPUTER

The dummy element FORTRAN source files and sample problems are provided on magnetic tape. The tape is written in VAX FILES-11 format and has the following characteristics.

1600 BPI
9 TRACK
ASCII

To install the code, all files should first be copied from the tape to either a user's disk space or to the system NASTRAN account disk space.

The following files, in order, will be found on the tape.

Dummy element stiffness and mass matrix routines

KDUM1.MIS

Dummy element thermal loads routines

DUM1.MIS

EDTL.MIS

Dummy element stress routines

SDUM11.MIS

SDUM12.MIS

Bulk data decks for sample problems

KITEST.NID

K12TEST.NID

To install the subroutines, they must be compiled and linked to the existing NASTRAN executable. Merge all the FORTRAN files (.MIS extensions) into one combined file called DUM1.TOT. The user must have available the two NASTRAN libraries, NASPRILIB.OLB and NASSECLIB.OLB. The following command procedure should be stored in a file called NC.COM and then executed by typing in @NC DUM1.TOT.

```
$SET NOON
$FORTRAN/NOF77 'P1'/OPTIMIZE/NOLIST/OBJECT=TEMPLIBR.OBJ
$KLIB:="NASPRILIB.OLB"
$LEN = 'F$LENGTH(P1)
$IF ('F$LOCATE(".VSS",P1) .NE. LEN) - THEN
    KLIB:="NASSECLIB.OLB"
$LIBRARY/REPLACE/LOG 'KLIB' TEMPLIBR.OBJ
$DELETE TEMPLIBR.OBJ;*
$SET ON
```

The above procedure compiles the source and inserts it into the old libraries. This procedure (NC.COM) and those that follow (LINK05.COM, etc.) are provided by COSMIC on the tapes containing the NASTRAN program. Refer to the "Supplemental Documentation for VAX NASTRAN" provided by COSMIC for further elaboration.

The following procedure links the object files created above and creates the executable NAST08.EXE. The following should be stored on a file called LINK08.COM and then executed by typing in @LINK08.

```
$LINK/NOMAP/EXE=NAST08.EXE NASPRILIB.OLB/INCLUDE=(NAST08),-
    NASSECLIB.OLB/INCLUDE=(VAX08,vax08e,1FTE2),-
    NASPRILIB.OLB/LIB/INCLUDE=-
    (GPTABD,XSFABD,SEMDBD,TABFBD,CN36BD)
$EXIT
```

The following procedure creates the executable NAST05.EXE. The following should be stored on a file called LINK05.COM and then executed by typing in @LINK05.

```
$LINK/NOMAP/EXE=NAST05.EXE  NASPRILIB.OLB/INCLUDE=(NAST05),-  
  NASSECLIB.OLB/INCLUDE=(VAX05,IFTE2),-  
  NASPRILIB.OLB/LIB/INCLUDE=-  
  (GPTABD,XSFABD,SEMDBD,CN36BD)  
$EXIT
```

Finally, the following procedure creates the executable NAST13.EXE. The following should be stored on a file called LINK13.COM and then executed by typing in @LINK13.

```
$LINK/NOMAP/EXE=NAST13.EXE  NASPRILIB.OLB/INCLUDE=(NAST13),-  
  NASSECLIB.OLB/INCLUDE=(VAX13,IFTE2,SETC),-  
  NASPRILIB.OLB/LIB/INCLUDE=-  
  (GPTABD,PLA4BD,XSFABD,SDR2BD,SEMDBD,- CN36BD)  
$EXIT
```

After executing the above procedures, three new files, NAST08.EXE, NAST05.EXE, and NAST13.EXE will be on the account. These are then to be used in place of the old NAST08.EXE, NAST05.EXE, and NAST13.EXE files which currently reside on the NASTRAN disk. If desired, the old NAST08.EXE, NAST05.EXE, and NAST13.EXE files may be deleted from the NASTRAN disk at this time.

The Bulk data decks KITEST.NID and K12TEST.NID for the sample problems are used in exactly the same manner as any other bulk data deck.